Published in final edited form as:

Nature. 2019 October ; 574(7779): 575–580. doi:10.1038/s41586-019-1678-1.

Metabolic regulation of gene expression by histone lactylation

Di Zhang[1,*], **Zhanyun Tang**[2,*], **He Huang**[1,6], **Guolin Zhou**[1], **Chang Cui**[1], **Yejing Weng**[1], **Wenchao Liu**[1], **Sunjoo Kim**[1], **Sangkyu Lee**[1,7], **Mathew Perez-Neut**[1], **Daniel Czyz**[3], **Rong Hu**[4], **Zhen Ye**[4], **Maomao He**[5], **Y. George Zheng**[5], **Howard Shuman**[3], **Jun Ding**[1], **Lunzhi Dai**[1,8], **Bing Ren**[4], **Robert G. Roeder**[2], **Lev Becker**[1,9,‡], **Yingming Zhao**[1,9,‡]

[1]Ben May Department for Cancer Research, The University of Chicago, Chicago, IL 60637, USA

[2]Laboratory of Biochemistry and Molecular Biology, The Rockefeller University, New York, NY 10065, USA

[3]Department of Microbiology, The University of Chicago, Chicago, IL 60637, USA

[4]Ludwig Institute for Cancer Research, University of California at San Diego, La Jolla, CA 92093, USA

[5]Department of Pharmaceutical and Biomedical Sciences, University of Georgia, Athens, GA, 30602, USA

[6]Present address: Shanghai Institute of Materia Medica, Chinese Academy of Sciences, Shanghai 201203, P.R. China

[7]Present address: BK21 Plus KNU Multi-Omics based Creative Drug Research Team, College of Pharmacy, Research Institute of Pharmaceutical Sciences, Kyungpook National University, Daegu, 41566, Republic of Korea

[8]Present address: Department of General Practice, State Key Laboratory of Biotherapy, West China Hospital, Sichuan University, and Collaborative Innovation Center of Biotherapy, Chengdu 610041, China

‡ Correspondence and requests for materials should be addressed to L.B. (levb@uchicago.edu) and Y.Z. (Yingming.Zhao@uchicago.edu).

*These authors contribute equally to this work

Author Contributions.

Y.Z. conceived the project and developed the general ideas and research strategy. D.Z., L.B., Y.Z designed the experimental approach and composed the manuscript. D.Z. performed most of the experiments. Z.T. and R.G.R. carried out *in vitro* chromatin-based transcription experiments. Y.W., H.H., W.L., J.D., L.D., S.K., and M.P. contributed to mass spectrometry related experiments and analysis; R.H., Z.Y. and B.R. performed the library construction and next-generation sequencing for ChIP-seq and RNA-seq; M.H. and Y.G.Z. synthesized L-lactyl-CoA. H.H. and D.Z. analyzed ChIP-seq and RNA-seq data. G.Z. provided all primary BMDM cell cultures. D.M.C. carried out the bacterial infection experiments, C.C. carried out TAM experiments.

Author Information.

Y.Z. is a founder, board member, advisor to, and inventor on patents licensed to PTM Bio Inc. L.B. is co-founder and CSO of rMark Bio Inc., and founder and CEO of Onchilles Pharma Inc. Readers are welcome to comment on the online version of the paper.

Data availability.

The ChIP-seq and RNA-seq data have been made available at the Gene Expression Omnibus (GEO) repository under the accession number GSE115354. The mass spectrometry proteomics data have been deposited to the ProteomeXchange Consortium via the PRIDE[31] partner repository with the dataset identifier PXD014870. All other data are available from the authors upon reasonable request.

[9]University of Chicago Medicine Comprehensive Cancer Center, Chicago, IL 60637, USA

Abstract

The Warburg effect, originally describing augmented lactogenesis in cancer, is associated with diverse cellular processes such as angiogenesis, hypoxia, macrophage polarization, and T-cell activation. This phenomenon is intimately linked with multiple diseases including neoplasia, sepsis, and autoimmune diseases[1,2]. Lactate, a compound generated during Warburg effect, is widely known as an energy source and metabolic byproduct. However, its non-metabolic functions in physiology and disease remain unknown. Here we report lactate-derived histone lysine lactylation as a new epigenetic modification and demonstrate that histone lactylation directly stimulates gene transcription from chromatin. In total, we identify 28 lactylation sites on core histones in human and mouse cells. Hypoxia and bacterial challenges induce production of lactate through glycolysis that in turn serves as precursor for stimulating histone lactylation. Using bacterially exposed M1 macrophages as a model system, we demonstrate that histone lactylation has different temporal dynamics from acetylation. In the late phase of M1 macrophage polarization, elevated histone lactylation induces homeostatic genes involved in wound healing including arginase 1. Collectively, our results suggest the presence of an endogenous “lactate clock” in bacterially challenged M1 macrophages that turns on gene expression to promote homeostasis. Histone lactylation thus represents a new avenue for understanding the functions of lactate and its role in diverse pathophysiological conditions, including infection and cancer.

Keywords

Epigenetics; histone marks; histones; hypoxia; lactate; lysine lactylation; macrophages; protein post-translational modifications; proteomics; Warburg effect

Inspired by the discovery of various histone acylations derived from cellular metabolites[3,4], we predicted and identified lysine lactylation (Kla) as a new type of histone mark that can be stimulated by lactate (illustrated in Fig. 1a). Initial evidence for histone Kla came from the observation of a mass shift of 72.021 Daltons on lysine residues in three proteolytic peptides that were detected in high performance liquid chromatography (HPLC)-tandem mass spectrometric (MS/MS) analysis of tryptically digested core histones from MCF-7 cells (Fig. 1b and Extended Data Fig. 1b, d). This mass shift is the same as that caused by addition of a lactyl group to the ε amino group of a lysine residue.

To validate the existence of lysine lactylation in histones, we used four orthogonal methods[5]. In the first two methods, we used HPLC-MS/MS to compare a synthetic peptide and its *in vivo*-derived counterpart to determine whether the two versions of the peptide have the same chemical properties in terms of chromatographic elution in HPLC and fragmentation pattern in MS/MS. To this end, we generated three histone peptides bearing Kla modifications: H3K23-QLATK_{la}AAR, H2BK5-PELAK_{la}SAPAPK, and H4K8-GGK_{la}GLGK. Each pair of peptides co-eluted in HPLC and had comparable MS/MS spectra (Fig. 1b and Extended Data Fig. 1a–e). To further confirm the modification, we developed a pan anti-Kla antibody (Extended Data Fig. 1f, g). Immunoblots using the pan anti-Kla antibody confirmed the presence of histone Kla and showed that histone Kla levels were elevated in a dose-

dependent fashion in response to exogenous L-lactate (Extended Data Fig. 1h–j). Subsequent MS analyses identified 26 and 16 histone Kla sites from human MCF-7 cells and mouse bone marrow-derived macrophages (BMDMs), respectively (Fig. 1c). Finally, metabolic labeling experiments using isotopic sodium L-lactate ($^{13}C_3$) followed by MS/MS analysis demonstrated that lysine lactylation can be derived from lactate (Extended Data Fig. 1k). Together, these experiments demonstrate that histone Kla is an *in vivo* protein post-translational modification derived from lactate.

Given that extracellular lactate can stimulate histone Kla, we hypothesized that modulation of intracellular lactate production would also impact histone Kla levels. We exposed MCF-7 and other cell lines to various concentrations of glucose, the major source of intracellular lactate. Both lactate production and histone Kla levels were induced by glucose in a dose-dependent manner (Fig. 2a, b, and Extended Data Fig. 2a–c). Conversely, 2-deoxy-D-glucose (2-DG), a non-metabolizable glucose analog, decreased both lactate production and histone Kla levels (Fig. 2c, d). Furthermore, metabolic labeling experiments using isotopic glucose (U-$^{13}C_6$) followed by MS/MS analysis demonstrated that lysine lactylation is endogenously derived from glucose (Extended Data Fig. 2d and Supplementary table 1). Quantitative proteomics analysis across a diverse set of histone sites demonstrated that histone Kla and Kac have different kinetics of ^{13}C glucose incorporation in MCF-7 cells (Extended Data Fig. 2e, f). ^{13}C labeled histone Kac reached a steady state at 6h, similar to the observation in HCT116 cells by Liu et al[6]. In contrast, histone Kla increased over a 24h time course (Extended Data Fig. 2e, f). Immunoblotting results corroborated the MS/MS data in MCF-7 as well as other cell lines (Extended Data Fig. 2i–k).

Lactate production is determined by the balance between glycolysis and mitochondrial metabolism. We tested whether the activities of enzymes in these two pathways can modulate lactate levels that in turn regulates histone Kla (illustrated in Fig. 2e). Sodium dichloroacetate (DCA) and oxamate were used to inhibit lactate production by modulating activities of pyruvate dehydrogenase (PDH) and lactate dehydrogenase (LDH), respectively. As anticipated, intracellular lactate levels were decreased by these two compounds (Fig. 2f) and histone Kla levels were lowered (Fig. 2g, h). Conversely, rotenone, an inhibitor of the mitochondrial respiratory chain complex I that drives cells towards glycolysis increased both intracellular lactate and histone Kla levels (Fig. 2f, i). Quantification of histone Kla and Kac marks by Stable Isotope Labeling with Amino Acids in Cell Culture (SILAC) and MS/MS analysis corroborated the immunoblot data from DCA- and Rotenone-treated MCF-7 cells (Extended Data Fig. 2l, m). Furthermore, U-$^{13}C_6$ glucose labeling experiments showed that the incorporation of ^{13}C into histone Kla but not Kac was decreased by DCA (Extended Data Fig. 2e–h). Together, these observations demonstrate that endogenous lactate production is a key determinant of histone Kla levels.

Elevated glycolysis and lactate production are coupled with diverse cellular processes. To investigate whether histone Kla is regulated by glycolysis under physiological conditions, we chose two model systems: hypoxia and M1 macrophage polarization. In response to hypoxia, cells reprogram their metabolism by inhibiting oxidative phosphorylation and enhancing glycolysis, stimulating the production of lactate[7]. Hypoxia induced intracellular lactate production and increased histone Kla but not Kac levels in MCF-7 cells (Fig. 2j, k,

and Extended Data Fig. 3a–d). SILAC-based mass spectrometric quantification of histone Kla and Kac confirmed the immunoblotting data (Extended Data Fig. 3e, f). Similar results were obtained in HeLa and RAW264.7 cells (Extended Data Fig. 3g, h). Furthermore, we found that the induction of lactate production and histone Kla by hypoxia were attenuated by an LDH inhibitor (Oxamate) or a PDK1 inhibitor (DCA) (Extended Data Fig. 3i, j). Deleting both *LDHA* and *LDHB* fully suppressed lactate production and histone Kla in HepG2 cells under normoxic conditions (Extended Data Fig. 3k, l). Due to poor cell viability, hypoxic conditions could not be tested (data not shown).

Emerging evidence shows that lactate has regulatory functions in both innate and adaptive immune cells[8] and induces dramatic changes in gene expression[9], suggesting that lactate is not simply a "waste product" of glycolysis. Pro-inflammatory M1 macrophages undergo metabolic reprogramming toward aerobic glycolysis, resulting in lactate production, whereas anti-inflammatory M2 macrophages trigger a metabolic program of increased oxidative phosphorylation and fatty acid oxidation[10]. Our discovery of histone Kla marks and their dynamics therefore suggests a role in regulating gene expression during M1 macrophage polarization.

To test this hypothesis, we examined the dynamics of lactate production and histone Kla marks during M1 macrophage polarization following treatment of BMDMs with lipopolysaccharide (LPS) and interferon-γ (IFN γ). We observed increased intracellular lactate levels 16 to 24 hours after M1 activation (Fig. 3a), which were well correlated with increased histone Kla levels (Fig. 3b, c). In contrast, histone Kac levels were decreased at these time points (Fig. 3b, c). This differential pattern was confirmed by U-$^{13}C_6$ glucose labeling experiments, which showed that ^{13}C labeled histone Kac peaked 3hr after labeling and declined to a steady state, while histone Kla increased over the 24h time course (Extended Data Fig. 4a–d). In addition, GNE-140, an LDHA specific inhibitor reduced ^{13}C incorporation into histone Kla, but not Kac (Extended Data Fig. 4e, f). The increase of histone Kla during M1 polarization is intrinsic and not due to paracrine effects, because replenishing cells with fresh media every 4 hours did not affect Kla levels (Extended Data Fig. 4g). Increases in lactate production and histone Kla are also specific to M1 macrophages because they were not observed in M2-polarized BMDMs (Fig. 3d and Extended Data Fig. 4h), which are more reliant on fatty acid oxidation[10].

Histone modifications play an important role in the regulation of gene expression[11]. To investigate histone Kla-associated genes 24 hours post-M1 polarization of macrophages, we performed RNA-seq and paired ChIP-seq using anti-H3K18la or anti-H3K18ac antibodies, whose specificities were validated by dot blots (Extended Data Fig. 3a–d), ChIP-qPCR assays (Extended Data Fig. 4i, j) and immunoblots (Extended Data Fig. 4k).

Our ChIP-seq data showed that H3K18la and H3K18ac were both enriched in promoter regions (± 2 kb around transcriptional start sites) (Extended Data Fig. 4l) and were indicative of steady-state mRNA levels (Extended Data Fig. 4m, n). In addition, elevated H3K18la (2-fold increase) marked more genes than decreased H3K18la (2-fold decrease), while the converse was true for the H3K18ac modification (Fig. 3e). Moreover, the majority of genes marked by elevated H3K18la were specific, since 68% of these genes (1223/1787) did not

display significantly elevated H3K18ac (Fig. 3e, f, and Supplementary Tables 2, 3). In contrast, no H3K18ac-specific genes were identified (Fig. 3e, f). Representative tracks from ChIP-seq studies are shown in Extended Data Fig. 4o, p.

To study correlations between H3K18la marks and gene expression, we performed RNA-seq 0, 4, 8, 16, and 24 hours after LPS/IFNγ challenge (Extended Data Fig. 5a and Supplementary Table 4). As expected, inflammatory response genes (*e.g.*, *Nos2*) were induced as early as 4 hours following LPS/IFNγ challenge, and their expression levels steadily declined at later time points (Fig. 3g). Interestingly, the 1223 genes specifically marked by elevated H3K18la were more likely to be activated or reactivated at later time points (16 or 24 hours) during M1 polarization (Fig. 3h and Extended Data Fig. 5a–c), which correlated well with the induction of intracellular lactate and histone Kla levels at these later time points (Fig. 3a–c). Gene Ontology (GO) analysis revealed that these H3K18la-specific genes were enriched in biological pathways independent of inflammation (Extended Data Fig. 5d). One of these enriched pathways was wound healing (*e.g.*, *Arg1*), which has been associated with the M2-like phenotype (Fig. 3h and Extended Data Fig. 5d). To corroborate these findings with more physiologically relevant stimuli, we treated BMDMs (M0) with live or dead gram-negative bacteria (*E. coli*, *A. baumannii*, and *P. aeruginosa*) to stimulate M1 polarization. Similar to LPS, bacteria induced lactate production and global histone Kla but not histone Kac levels (Fig. 3i and Extended Data Fig. 5e, f), and kinetics of early cytokine and late *Arg1* expression were maintained (Fig. 3j, and Extended Data Fig. 5g–j).

Arginine metabolism is a key catabolic and anabolic process that is regulated during macrophage polarization. M1 macrophages are thought to have low ARG1 and to metabolize arginine to produce nitric oxide through nitric oxide synthase to kill pathogens, while M2 macrophages have high ARG1 which produces ornithine to facilitate wound healing[12]. Consistent with their RNA dynamics, ARG1 protein levels and activity were significantly increased 24–48 hours post-M1 polarization, while NOS2 protein levels and function peaked 12 hours post-M1 polarization and declined at later time points (Fig. 3k and Extended Data Fig. 5k). Collectively, these findings suggest that induction of lactate during M1 activation might promote a late-phase switch to a more homeostatic phenotype, which shares some similarity with the M2-like phenotype. Indeed, previous studies showed that treating BMDMs with tumor cell-derived lactate drives an M2-like phenotype characteristic of tumor-associated macrophages (TAMs)[13]. Using murine cancer models, we observed a positive correlation between *Arg1* expression and histone Kla levels, but not histone Kac levels in TAMs isolated from B16F10 melanoma and LLC1 lung tumors (Extended Data Fig. 6a–e).

Changes in gene expression during M1 polarization are caused by complex signaling cascades induced by LPS/IFNγ, including the induction of lactate and histone Kla. To substantiate the role of lactate and histone Kla in the regulation of gene expression, we manipulated levels of lactate during M1 polarization and examined its effect on expression of *Arg1*, a M2-like gene. We first lowered lactate levels by deleting *Ldha* (LysM-Cre $^{+/-}$*Ldha*$^{fl/fl}$, Extended Data Fig. 7a–c). Lactate production and global histone Kla levels were both decreased in LDHA-deficient macrophages during M1 polarization (Fig. 4a, b).

Although deleting *Ldha* in macrophages did not alter proinflammatory cytokine expression (Extended Data Fig. 7d–g), it attenuated *Arg1* and decreased histone Kla marks at the *Arg1* promoter (Fig. 4c, d). Similar findings were obtained when macrophages were M1 polarized in the presence of the glycolysis inhibitors (2-DG, DCA and GNE-140) (Extended Data Fig. 7h–m). Next, we elevated lactate levels by treating M1 macrophages with exogenous lactate. Exogenous lactate increased intracellular lactate (Fig. 4e) and histone Kla levels (Fig. 4f), and induced *Arg1* expression (Fig. 4g) and Kla levels at the *Arg1* promoter (Fig. 4h). In contrast, exogenous lactate did not affect early pro-inflammatory gene expression (Extended Data Fig. 8a–d). In addition, exogenous lactate enhanced expression of other M2-like genes, such as *Vegfa* during M1 polarization (Extended Data Fig. 8e–h and Supplementary Table 5). Thus, this data confirmed the positive role of lactate and histone Kla in driving expression of M2-like genes during M1 macrophage polarization.

Our observed correlations between lactate, H3K18la, and M2-like gene expression does not necessarily imply that the histone Kla mark was a causative factor. Previous studies showed that exogenous lactate can alter *Arg1* and *Vegfa* expression in unstimulated (M0) macrophages through HIF1a[13]. However, HIF1a is unlikely to be important for regulating *Arg1* and *Vegfa* during M1 polarization as HIF1a protein was induced at early time points and HIF1a bound to promoters of glycolytic genes but not *Arg1* and *Vegfa* (Extended Data Fig. 8i–m).

To examine whether histone Kla plays a direct role in transcriptional regulation, we took advantage of a cell-free, recombinant chromatin-templated histone modification and transcription assay (Extended Data Fig. 9a) that was used previously to demonstrate direct transcriptional activation by p53- and p300-dependent histone Kac[14]. This assay, in which acetyl-CoA was replaced by L-lactyl-CoA (validated by HPLC and MS (Extended Data Fig. 9h–k)), demonstrated robust p53-dependent, p300-mediated H3 and H4 lactylation (Extended Data Fig. 9b) and a corresponding effect on transcription (Extended Data Fig. 9c). The effects paralleled those observed for acetyl-CoA dependent-histone acetylation and transcription. To confirm that transcription was directly mediated by lactylation of histones, rather than other proteins in the nuclear extract, recombinant chromatin was reconstituted with core histones bearing lysine (K) to arginine (R) mutations in histone tails[15]. Compared to wild type histones, the H3 and H4 mutations, but not the H2A or H2B mutations, eliminated p300- and p53-dependent transcription (Extended Data Fig. 9d). Taken together, these findings suggest that histone lactylation, like histone acetylation, can directly promote gene transcription under the described conditions. To examine the potential activity of p300 as a histone Kla writer in cells, we over-expressed p300 in HEK293T cells and observed a modest increase in histone Kla levels (Extended Data Fig. 9e). In contrast, p300 deletion in HCT116 and HEK293T cells decreased histone Kla levels (Extended Data Fig. 9f, g). Although we cannot exclude an indirect effect by p300 in these cells, together with the *in vitro* enzymatic results, these data suggest that p300 is a potential histone Kla writer protein.

In response to bacterial infection, macrophages must react rapidly with a substantial pro-inflammatory burst to help kill bacteria and recruit additional immune cells to the infection site. During this process, macrophages switch to aerobic glycolysis[10], which is thought to support pro-inflammatory cytokine expression during M1 activation[16] and produce the

Warburg effect. Over time, this metabolic switch also increases intracellular lactate, which we show stimulates histone lysine lactylation 16–24 hours after exposure to M1-polarizing stimuli. Histone lactylation is not required for the induction or suppression of pro-inflammatory genes. Instead, it serves as a mechanism to initiate expression of homeostatic genes that have been traditionally associated with M2-like macrophages. Our studies support a model wherein the switch to aerobic glycolysis that occurs during M1 polarization starts a "lactate timer" that uses an epigenetic mechanism to induce M2-like characteristics in the late phase, perhaps to assist with repairing collateral damage incurred by the host during infection.

High levels of lactate (e.g., 40 mM in certain type of tumor tissue[17]) is also associated with major hallmarks of cancer and other diseases. Given that the Kla modification can be stimulated by lactate and contribute to gene expression, the Kla modification will likely fill an important knowledge gap in our understanding of diverse physiopathology (e.g., infection, cancer) with which lactate is intimately associated.

Methods

Materials.

Pan anti-Kac (PTM-101), pan anti-Kla (PTM-1401), anti-H3K18la (PTM-1406), anti-H4K5la (PTM-1407), and anti-H4K8la (PTM-1405) antibodies were generated by PTM Bio Inc (Chicago, IL); anti-histone H3 (ab12079), anti-H3K18ac (ab1191) and anti-H3K27ac (ab4729) antibodies were purchased from Abcam (Cambridge, MA); *Drosophila* spike-in antibody (61686) and spike-in chromatin (53083) were obtained from Active Motif (Carlsbad, CA); anti-LDHA (2012S) antibody was from Cell Signaling Technology, Inc (Danvers, MA); anti-α-Tubulin (05–829) and anti-LDHB (ABC927) antibodies were from Millipore Sigma (Burlington, MA); anti-HIF-1a (NB100–105) antibody was from Novus Biologicals (Littleton, CO); anti-iNOS (GTX130246) and anti-Arg1(GTX109242) antibodies were purchased from GeneTex (Irvine, CA); anti-p300 (sc-584) was from Santa Cruz Biotechnology, Inc (Dallas, TX); anti-CD11b Monoclonal Antibody (M1/70), PE-Cyanine7 (25-0112-82) and anti-F4/80 Monoclonal Antibody (BM8), APC (17-4801-82) were from ThermoFisher Scientific (Waltham, MA); lipopolysaccharides from *Escherichia coli* O111:B4 (L4391), sodium L-lactate (71718), L-(+)-lactic acid (L6402), sodium dichloroacetate (347795), Cobalt(II) chloride hexahydrate (C8661), rotenone (R8875), and acetyl coenzyme A (A2056) were purchased from Sigma-Aldrich (St. Louis, MO); sodium L-lactate (13C3, 98%) (CLM-1579-PK) and D-glucose (U-13C6, 99%) (CLM-1396-1) were purchased from Cambridge Isotope Laboratories (Andover, MA). Recombinant mouse IFN-γ protein (485-MI-100) was from R&D Systems (Minneapolis, MN); mouse interleukin-4 (130-097-760) was from Miltenyi Biotec (Bergisch Gladbach, Germany); modified sequencing-grade trypsin was from Promega (Madison, WI); lactate colorimetric assay kit II (K627–100), arginase activity colorimetric assay kit (K755–100), and nitric oxide synthase (NOS) activity assay kit (K205–100) were purchased from Biovision, Inc (Milpitas, CA).

Cell Culture.

MCF-7, MDA-MB-231, HeLa, A549, HepG2, MEF, and RAW 264.7 cells were obtained from the American Type Culture Collection and cultured in Dulbecco's modified Eagle's medium supplemented with 10% FBS and 1% GlutaMAX (GIBCO, Gaithersburg, MD). Cells were routinely tested for mycoplasma contamination (MP0035, Sigma-Aldrich, St. Louis, MO), and only negative cells were used in experiments. No specific cell line authentication was performed. For growth under hypoxic conditions, cells were grown in a specialized, humidified chamber equilibrated with 1% oxygen / 94% nitrogen / 5% carbon dioxide for the indicated time.

Mouse experiments.

All animal use and experiments performed were approved by Institutional Animal Care and Use Committee (ACUP#72209) at the University of Chicago. *Ldha*$^{fl/fl}$ mice (Jackson laboratory, 030112) and LysMcre mice (Jackson laboratory, 004781) were used to generate LysMcre$^{+/-}$ *Ldha*$^{fl/fl}$ and littermate control LysMcre$^{-/-}$ *Ldha*$^{fl/fl}$ mice. The following primers were used for genotyping: Ldha forward: CTGAGCACACCCATGTGAGA and Ldha reverse: AGCAACACTCCAAGTCAGGA. LysMcre: CCCAGAAATGCCAGATTACG, LysM Common: CTTGGGCTGCCAGAATTTCTC and LysM WT: TTACAGTCGGCCAGGCTGAC. Macrophages were derived from bone marrow of 8-week male C57BL/6 mice following the published procedure[18]. To induce an M1 or M2 phenotype, BMDM cells were stimulated with 5 ng/ml of LPS and 12 ng/ml of IFNγ, or 20 ng/ml of interleukin 4, for 24 hours or the indicated time. To infect BMDM cells with bacteria, overnight cultures of *E. coli*, *A. baumannii*, or *P. aeruginosa* were diluted in RPMI-1640 and added to BMDM cells in 6-well plates at 2 and 20 multiplicity of infection. A control plate was either infected with paraformaldehyde-killed bacteria or treated with 5 ng/mL lipopolysaccharide (LPS) in the absence of bacteria. The plates were centrifuged at 2170 rpm for 30 min to promote infection, followed by a 30 min incubation in a humidified incubator at 37°C under 5% CO_2. To kill extracellular bacteria, the medium overlying the confluent cell monolayer was replaced with fresh media containing gentamicin at 100 μg/mL and the plates were further incubated for 1 h. Following incubation, media were removed from infected cells and replaced with fresh media containing 25 μg/mL of gentamicin. For consistency, LPS-treated cells and cells infected with dead bacteria were also treated with gentamicin. Cells were cultured for 24 h before lysis. Allocation of BMDM cells into different treated groups were randomized and not blinded.

Tumor inoculation and Tumor-associated macrophages (TAMs) isolation.

LLC1 cells (0.5×10^6) or B16F10 cells (1×10^6) were injected into 7 weeks old C57BL/6 mice (The Jackson Laboratory). Once tumors reached ~ 600 mm^3, mice were sacrificed for tumor isolation. Tumors were digested with Type 4 Collagenase (Worthington, 3 mg/mL) and hyaluronidases (Sigma, 1.5 mg/mL) in 1% BSA/PBS at 37°C with shaking at 200 rpm for 30 min. The digested tumor was then filtered through a 70-um cell strainer, followed by RBC lysis step and passing through another 40-um strainer. Cells were resuspended into isolation buffer (0.1% BSA/PBS, 2 mM EDTA), layered onto Ficoll-PaqueTM PLUS (GE Healthcare), and centrifuged at 450 g for 30 mins without break. Mononuclear immune cells

were obtained by taking out the middle white layer. TAMs were then isolated using CD11b Microbeads (Mitenyi Biotec) as company instructed. TAMs' purity was confirmed by flow cytometry using CD11b and F4/80 antibody. Data were quantified by FlowJo v.10.4.1.

Peptide Immunoprecipitation.

Histones from human MCF-7 or mouse BMDM cells were extracted using a standard acid extraction protocol[19], and subjected to trypsin digestion as per the manufacturer's instructions. Pan anti-Kla or pan anti-Kac antibodies were first conjugated to nProtein A Sepharose beads (GE Healthcare BioSciences, Pittsburgh, PA) and then incubated with tryptically digested histone peptides with gentle agitation overnight at 4 °C. The beads were then washed three times with NETN buffer (50 mM Tris-Cl pH 8.0, 100 mM NaCl, 1 mM EDTA, 0.5% NP-40), two times with ETN buffer (50 mM Tris-Cl pH 8.0, 100 mM NaCl, 1 mM EDTA) and once with water. Peptides were eluted from the beads with 0.1% TFA and dried in a SpeedVac system (Thermo Fisher Scientific, Waltham, MA).

HPLC/MS/MS analysis.

The peptide samples were loaded onto a home-made capillary column (10 cm length × 75 mm ID, 3 μm particle size, Dr. Maisch GmbH, Ammerbuch, Germany) connected to an EASY-nLC 1000 system (Thermo Fisher Scientific, Waltham, MA). Peptides were separated and eluted with a gradient of 2% to 90% HPLC buffer B (0.1% formic acid in acetonitrile, v/v) in buffer A (0.1% formic acid in water, v/v) at a flow rate of 200 nL/min over 60 min (34 min for coelution studies). The eluted peptides were then ionized and analyzed by a Q-Exactive mass spectrometer (Thermo Fisher Scientific, Waltham, MA). Full MS was acquired in the Orbitrap mass analyzer over the range m/z 300–1400 with a resolution of 70,000 at m/z 200. The 12 most intense ions with charge ≥2 were fragmented with normalized collision energy of 27 and tandem mass spectra were acquired with a mass resolution of 17500 at m/z 200.

Isotopic labeling experiments.

MCF-7 cells were cultured in DMEM high glucose media plus 10% FBS. To be labeled by isotopic lactate, cells were treated with 10 mM of $^{13}C_3$ sodium L-lactate for 24 hours. To be labeled by isotopic glucose, cells were switched to DMEM No-Glucose media (Gibco) for 24 hours, followed by supplementation with 25 mM of U-$^{13}C_6$ D-glucose and continued culturing for three passages. Histones were extracted, digested with trypsin, immunoprecipitated using a pan anti-Kla antibody, and analyzed by HPLC/MS/MS as described above.

SILAC-based quantification.

MCF-7 cells were cultured in either "heavy" (L-Lysine-$^{13}C_6$, $^{15}N_2$) or "light" (L-Lysine-$^{12}C_6$, $^{14}N_2$) DMEM, supplemented with 10% dialyzed FBS (Serum Source International Inc, Charlotte, North Carolina), for more than six passages, to achieve more than 99% labeling efficiency. "Heavy" labeled and "light" labeled cells were mixed in a 1:1 ratio. Histones were extracted, digested with trypsin, immunoprecipitated using a pan anti-Kla antibody, and analyzed by HPLC/MS/MS as described above. Quantification was

analyzed by Maxquant[20]. Ratio H/L derived from Maxquant was then normalized by protein abundance.

Synthesis of L-lactyl-CoA.

L-Lactic acid (90 mg, 1 mmol) was dissolved in 5 mL of freshly distilled CH_2Cl_2. To this solution was added N-hydroxysuccinimide (115 mg, 1mmol), the reaction mixture was sonicated to obtain a clear solution. Then N,N'-Dicyclohexylcarbodiimide (DCC, 227 mg, 1.1 mmol) was added in one portion. A white precipitate formed upon addition. The reaction mixture was stirred at r.t. overnight. Then the white precipitate was filtered and washed with CH_3CN. The resulting organic solvent was evaporated by vacuum to afford crude product L-lactyl-NHS (170mg, 91% yield), which was used in the next step without further purification. 0.0065 mmol of CoA hydrate (5 mg) was dissolved in 1.5 mL of 0.5 M $NaHCO_3$ (pH 8.0) and cooled down on ice bath. Then L-lactyl-NHS (2.5 mg, 0.013 mmol) in 0.5 mL of CH_3CN/Acetone (1:1 v/v) was added dropwise to the CoA solution. The reaction solution was stirred at 4 °C overnight and then quenched by adjusting pH to 4.0 with 1.0 M HCl. The reaction mixture was then subjected to RP-HPLC purification with gradient 5–45% Buffer A in Buffer B over 30 min at flow rate 5 mL/min; UV detection wavelength was fixed at 214 and 254 nm (HPLC buffer A: 0.05% TFA in water; HPLC buffer B: 0.05% TFA in acetonitrile). The fractions were collected and lyophilized after flash-freeze with liquid nitrogen. m=2 mg, yield 38% ^{1}H NMR (400 MHz, Deuterium Oxide) δ 8.57 (s, 1H), 8.33 (s, 1H), 6.12 (d, J = 5.7 Hz, 1H), 4.49 (s, 1H), 4.29 – 4.24 (m, 1H), 4.14 (s, 2H), 3.93 (s, 1H), 3.75 (d, J = 8.6 Hz, 1H), 3.48 (d, J = 7.6 Hz, 1H), 3.35 (t, J = 6.4 Hz, 2H), 3.22 (d, J = 5.2 Hz, 3H), 2.89 (q, J = 6.2 Hz, 2H), 2.32 (t, J = 6.4 Hz, 2H), 1.23 (d, J = 6.9 Hz, 3H), 0.83 (s, 3H), 0.70 (s, 3H). MALDI m/z calcd. for $C_{24}H_{41}N_7O_{18}P_3S^+$ [M + H]$^+$: 840.1, found 839.6.

In *vitro* chromatin template-based histone modification and transcription assays.

Purification of recombinant proteins and chromatin assembly were performed as previously described[15]. The chromatin-templated histone modification and transcription assays were as described previously[15], except that lactyl-CoA was used in place of acetyl-CoA and [α-32P] CTP was used in place of [α-32P]-UTP. The H3KR, H4KR, H2AKR, and H2BKR histone mutants were the same as previously described[15]. Histone modifications were monitored by immunoblot and transcription products were monitored by autoradiography as described[15].

RNA-seq.

Total RNA was extracted from BMDM cells activated as indicated using a RNeasy Plus Mini Kit (74134, Qiagen, Hilden, Germany). Two to four micrograms of total RNA were used as starting material to prepare libraries using Illumina TruSeq Stranded mRNA Library Prep Kit Set A (RS-122–2101, Illumina, San Diego, CA). The libraries' size was selected by using the Agencourt AMPure XP beads (A63882, Beckman Coulter, Brea, CA), with average size of 400 bp. The libraries were sequenced using Illumina HiSeq 4000 (pair end 50 bp).

Bioinformatic analysis of RNA-seq data: Sequencing quality was evaluated by FastQC version 0.11.4. All reads were mapped to the reference genome of Illumina iGenomes UCSC

mm10 using HISAT2 version 2.1.0[21]. Differential expression analysis was implemented using edgeR version 3.16.5[22], after retaining only genes for which counts per million (cpm) was larger than one in four samples and normalizing the library sizes across samples using the TMM method of the edgeR package. Hierarchical clustering was performed and heat maps were generated using Perseus version 1.6.1.1 (http://www.coxdocs.org/doku.php?id=perseus:start). The Log2 transformed gene expression values (Reads Per Kilobase of transcript, per Million mapped reads (RPKM)) were normalized by subtracting the mean in every row, and hierarchically clustered with a Pearson correlation algorithm. Gene Ontology analysis (GOTERM_BP_DIRECT) was carried out using DAVID Bioinformatics Resources 6.8[23,24].

The following primers were used for RT-qPCR analysis: *Arg1*: CTCCAAGCCAAAGTCCTTAGAG, AGGAGCTGTCATTAGGGACATC; *Vegfa*: CCACGACAGAAGGAGAGCAGAAGTCC, CGTTACAGCAGCCTGCACAGCG; *Il6*: GTTCTCTGGGAAATCGTGGA, TTTCTGCAAGTGCATCATCG; *Il1b*: TTTGACAGTGATGAGAATGACC, CTCTTGTTGATGTGCTGCTG; *Ifnb1*: CAGCTCCAAGAAAGGACGAAC, GGCAGTGTAACTCTTCTGCAT; *Cxcl10*: CCAAGTGCTGCCGTCATTTTC, GGCTCGCAGGGATGATTTCAA; *Tnfa*: CCCTCACACTCAGATCATCTTCT, GCTACGACGTGGGCTACAG

ChIP-seq.

Native ChIP was carried out following the published protocol[25] with spiked-in for normalization purpose. Spike-in was carried out according to vendor protocols (# 61686, Active motif, Carlsbad, CA). Briefly, 50 ng of Spike-in chromatin (# 53083, Active motif, Carlsbad, CA) was added to 25 μg of BMDM chromatin to incubate with 2 μg Spike-in antibody (# 61686, Active motif, Carlsbad, CA) together with 4 μg of anti-H3K18la or anti-H3K18ac antibodies. After 4 hours of incubation at 4 °C, Protein A Sepharose (17-5280-01, GE Healthcare Life Sciences, Pittsburgh, PA) was added and incubated for another 2 hours, followed by sequential wash with buffer TSE I (0.1% SDS, 1% Triton X-100, 2 mM EDTA, 20 mM Tris-HCl pH 8.0, 150 mM NaCl), TSE II (0.1% SDS, 1% Triton X-100, 2 mM EDTA, 20 mM Tris-HCl pH 8.0, 500 mM NaCl), buffer III (0.25 M LiCl, 1% NP-40, 1% deoxycholate, 1 mM EDTA, 10 mM Tris-HCl pH 8.0), and TE buffer (1 mM EDTA, 10 mM Tris-HCl pH 8.0). Chromatin DNA was finally eluted with buffer containing 1% SDS and 0.1 M $NaHCO_3$. The eluates were digested with RNase A (12091021, Thermo Fisher Scientific, Waltham, MA) and proteinase K (AM2546, Thermo Fisher Scientific, Waltham, MA). DNA was recovered using the QIAquick PCR purification kit (#28106, Qiagen, Hilden, Germany) according to the manufacturer's instructions.

ChIP-seq libraries were constructed with an Accel-NGS 2S Plus DNA Library Kit (Swift Biosciences, Ann Arbor, MI) according to the manufacturer's protocol. The libraries were then amplified and assessed for fragment size using TapeStation (Agilent, Santa Clara, CA) and quantified using a Qubit dsDNA HS Assay Kit (Thermo Fisher Scientific, Waltham, MA). The indexed libraries were pooled and sequenced on a Hiseq4000 Sequencer (Illumina, San Diego, CA) using the 50-nt single-read configuration.

Bioinformatics analysis of ChIP-seq data: Sequencing quality was evaluated by FastQC version 0.11.4. All reads were mapped to the reference genome of Illumina iGenomes UCSC mm10 using Bowtie version 2.2.6[26,27], and only uniquely mapped reads were retained. Then SAMtools version 0.1.19[28] was used to convert files to bam format, sort, and remove PCR duplicates. Peaks were called using MACS version 2.2.1[29] under q value = 0.01. To quantify and directly compare H3K18la or H3K18ac in different samples (M0 and M1 macrophages), the uniquely mapped H3K18la or H3K18ac reads in promoter regions (± 2 kb around transcriptional start sites) of each gene were counted by featureCounts version 1.5.0-p1[30], and then normalized by Spike-in ChIP read counts of the corresponding condition (M0 or M1 macrophages). The overlap genes in ChIP-seq and RNA-seq data were used for all subsequent analysis. Gene Ontology analysis (GOTERM_BP_DIRECT) was carried out using DAVID Bioinformatics Resources 6.8[23,24].

The following primers were used for qPCR analysis of gene promoter regions in human cells:

FOXO3a-promoter: CAGTGAGTGTGTGCAGCTTG, AAAGCCTCCTGTTTGTGCTT; *FOXO3a*-downstream: TGCACACAGAAGCCAGAAG, GCTCCCCACAGAGACGTAA; *LDHA*-promoter: TAAGGGTGGGGGATACCTCT, CCCAAGAGAAAAATGCAAGC. The following primers were used for qPCR analysis of gene promoter regions in mouse cells: *Arg1*/*Arg1*-PTM: AAGCTGTGGCCTCAGAACAT, GGTAACCGCTGTGAAAGGAT; *Arg1*-HRE-1kb: CCCGAGTTTGACCCGAAGAA, CTTTACACAGGGACCGGACC; *Arg1*-HRE-2kb: TGTCTCTCCCAGTTTCCCCA, AGCAACTTGGCATCTGATGGA; *Vegfa*/*Vegfa*-PTM: CGAGCTAGCACTTCTCCCAG, AACTTCTGGGCTCTTCTCGC; *Vegfa*-HRE-1kb: GGCACCAAATTTGTGGCACT, CTGCCAGACTACACAGTGCA; *Vegfa*-HRE-2kb: ACCTGATCCTGATCCCTGCT, CAGCCTCTGTTATGCCACGA; *Vegfa*-HRE-3kb: GCAGAACCTAGGCTTCACGT, TTGAAAGGGCTGACATGGCT; *Eno1*: AAGGTCATCAGCAAGGTCGT, CGTACTCCGAGTCTCACACG; *Glut1*(*Slc2a1*): TAGATCCCCTCCCTCTTGCT, GAACACGTAGCCTGCTCACA; Gene desert: CTGCCAGGGTTGTAGAGAGG, GCCAGATCATATTGGCTTGG.

Statistical analysis.

No statistical methods were used to predetermine sample size. The significance of differences in the experimental data were determined using GraphPad Prism 7.0 software. All data involving statistics are presented as mean ± s.e.m. For data presented without statistics, experiments were repeated at least three times to ensure reproducibility, unless otherwise stated.

Extended Data

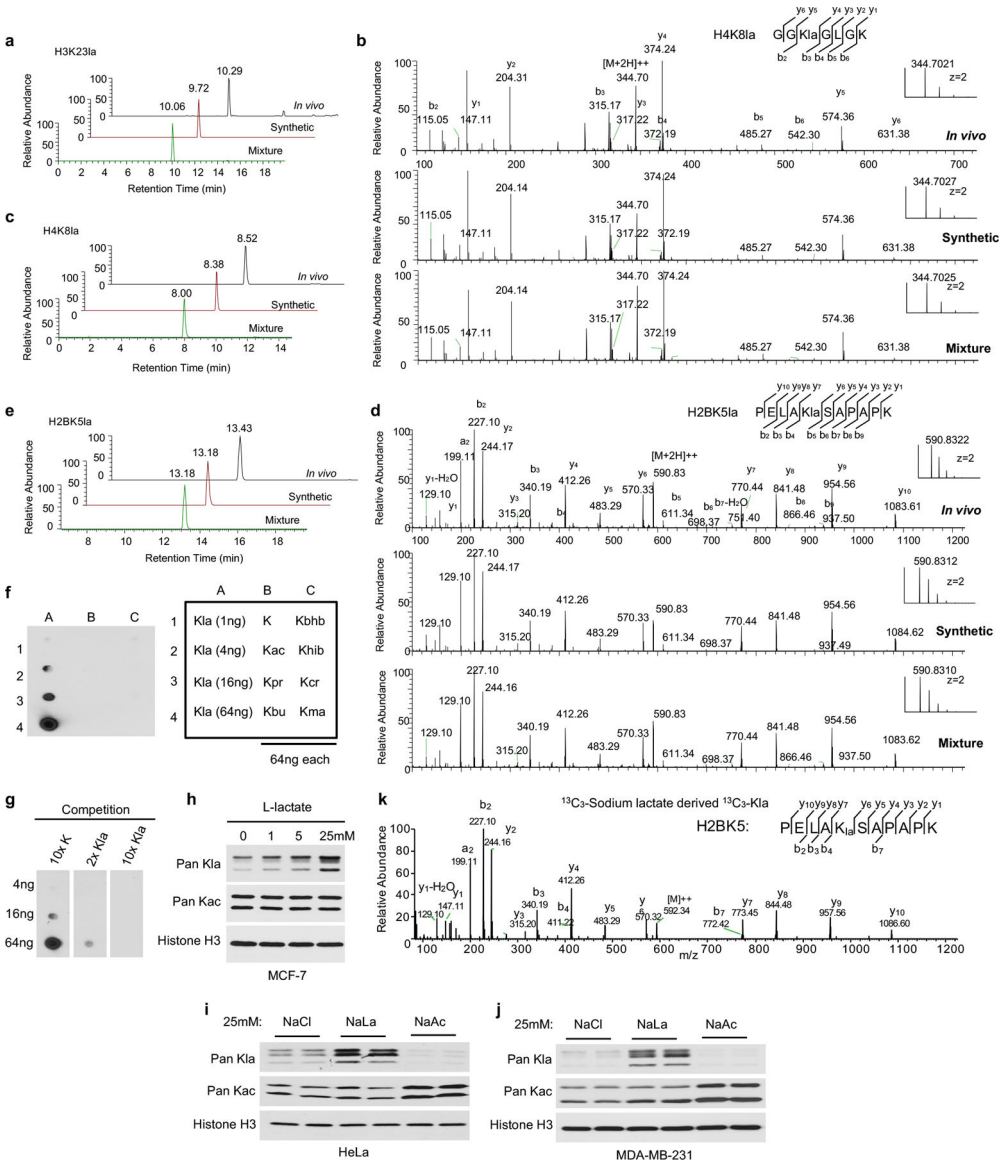

Extended Data Figure 1. Validation of histone lysine lactylation.

a, **c, e,** Extracted ion chromatograms from HPLC/MS/MS analysis of histone Kla peptides derived from cultured cells (*in vivo*), the synthetic counterparts, and their mixtures. **b, d,** MS/MS spectra of histone Kla peptides derived from *in vivo*, the synthetic counterparts, and their mixtures. **f, g,** Antibody specificity tests by dot blot and competition assay. **f,** Dot blot was carried out with a pan anti-Kla antibody and the following peptide libraries: A1–A4: Dots contain 1, 4, 16, and 64 ng, respectively, of a peptide library containing a lactylated lysine residue. B1–B4: Dots contain 64 ng of a peptide library containing an unmodified (K), acetylated (Kac), propionylated (Kpr), and butyrylated (Kbu) lysine residue, respectively. C1–C4: Dots contain 64 ng of a peptide library containing a β-hydroxybutyrylated (Kbhb), 2-hydroxyisobutyrylated (Khib), crotonylated (Kcr), and malonylated (Kma) lysine residue, respectively. The libraries contained a mixture of CXXXKXXXX peptides, where C is cysteine, × is a mixture of all 19 amino acids except

for cysteine, and K is lysine with or without the indicated modifications. **g,** Competition was carried out by incubating the pan anti-Kla antibody with a 2-fold or 10-fold excess of the indicated peptide libraries before the dot blot assay. **h–j,** Exogenous lactate boosts histone Kla levels. Immunoblot analysis of histone Kla and Kac from human MCF-7, HeLa and MDA-MB-231 cells, respectively, treated with indicated chemicals. **k,** MS/MS spectra of an isotopically labeled histone Kla peptide identified from MCF-7 cells cultured with 10 mM isotopic ($^{13}C_3$) sodium L-lactate for 24 hours. **a–k** represent three independent experiments.

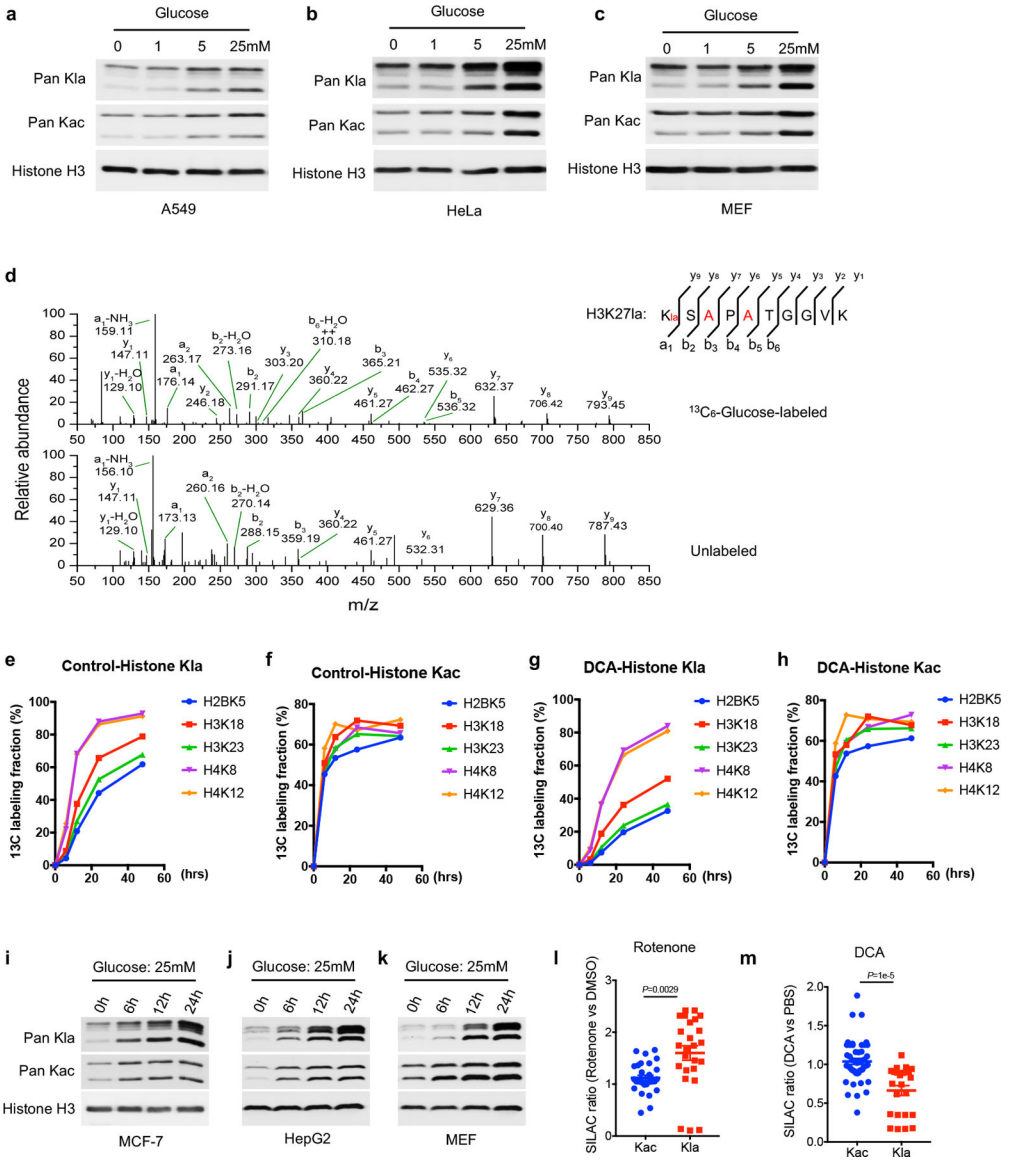

Extended Data Figure 2. Histone Kla is modulated by glycolysis pathway.

a–c, A549 (**a**), HeLa (**b**), and MEF (**c**) cells were cultured with indicated doses of glucose for 24h, without pyruvate. Histone Kla and Kac were analyzed by immunoblots using indicated antibodies. **d**, MS/MS spectra of a $^{13}C_6$-glucose labeled histone Kla peptide and its unlabeled counterpart from MCF-7 cells. **e–h,** Quantitative proteomic analysis of histone extracts from MCF-7 cells cultured in the presence of U-$^{13}C_6$ glucose for 6h, 12h, 24h, and 48h, with or without 10mM DCA. **i–k,** Histone Kla and Kac levels were analyzed by immunoblots using whole cell lysates from MCF-7, HepG2 and MEF cells exposed to 25 mM glucose for indicated time points. **l, m,** SILAC-MS/MS quantification of histone Kla and Kac marks from MCF-7 cells, comparing Rotenone (10 nM, 24h) vs DMSO (**l**), DCA (10mM, 24h) vs PBS (**m**). SILAC ratio was normalized to protein abundance. Each dot in the scatter dot plot represents one identified peptide from core histone. Graphs show mean ± s.e.m. **l**, Kac:1.121 ± 0.05084, n=31; Kla: 1.599 ± 0.139, n=25. **m**, Kac: 1.038 ± 0.03813,

n=49; Kla: 0.6627 ± 0.06376, n=24. Statistical significance was determined using Welch's t test (Two tailed). **a–d, i–k,** Data represent three independent experiments. **e–h,** Data represent two independent experiments.

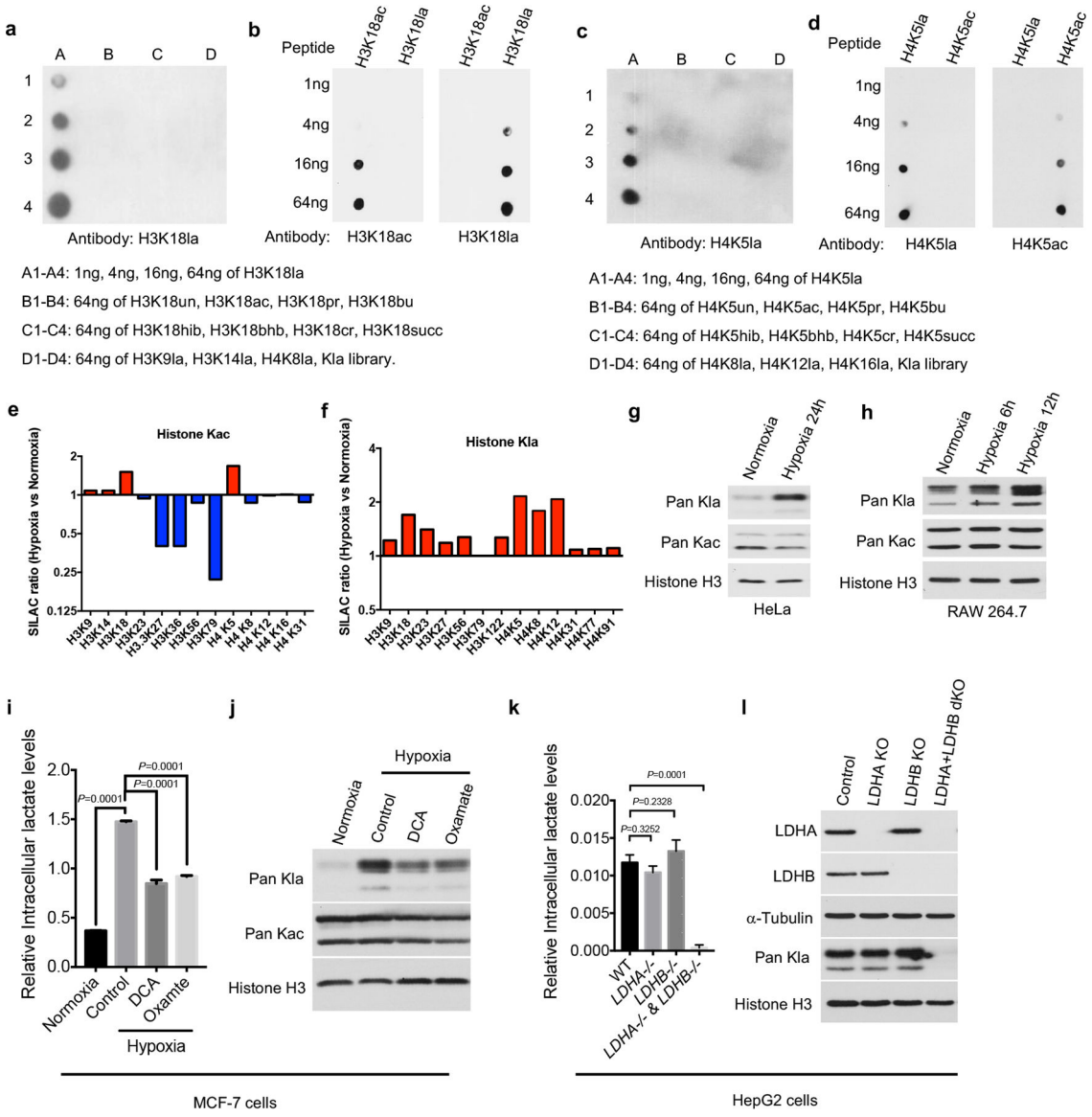

Extended Data Figure 3. Histone Kla is induced by hypoxia.

a–d, Antibody specificity was analyzed by dot blot assay. un: unmodified lysine; ac: acetyl lysine; pr: propionyl lysine; bu: butyryl lysine; hib; 2-hydroxyisobutyryl lysine; bhb: β-hydroxybutyryl lysine; cr: crotonyl lysine; succ: succinyl lysine. The Kla library was the same as the one used in Extended Data Fig. 1f. **e, f,** SILAC-MS/MS quantification of histone Kla and Kac marks from MCF-7 cells, comparing hypoxic (1% oxygen for 24 h) and normoxic conditions. SILAC ratio was normalized to protein abundance. **g, h,** Immunoblots of histone Kla and Kac from human HeLa and mouse RAW264.7 cells in response to hypoxia (1% oxygen) at the indicated time. **i**, **j**, Intracellular lactate (**i**) and histone Kla levels (**j**) were measured in MCF-7 cells comparing normoxia, hypoxia (1% oxygen, 24hrs), hypoxia in the presence of 10mM oxamate or 10mM DCA. **k**, **l,** Intracellular lactate (**k**) and histone Kla levels (**l**) were measured comparing *LDHA−/−*, *LDHB−/−*, or *LDHA−/− & LDHB−/−* with wildtype HepG2 cells. Graphs show mean with s.e.m. from three biological

independent samples; statistical significance was determined using one-way ANOVA followed by Dunnett's multiple comparisons test. **a–d, g, h, k,** and **l** represent three independent experiments.

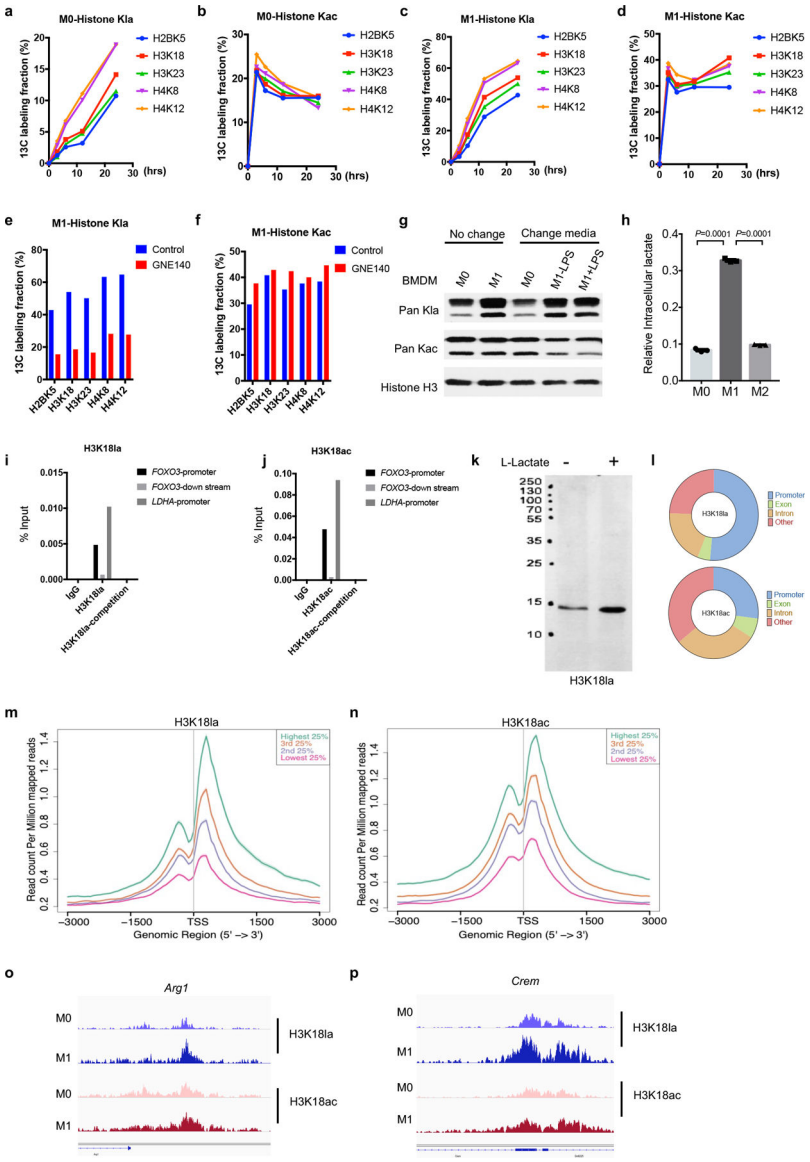

Extended Data Figure 4. Histone Kla is induced during M1 macrophage polarization.

a–f, Quantitative proteomic analysis of histone extracts from M0 and M1 macrophages (BMDM) cultured in the presence of U-$^{13}C_6$ glucose for 3h, 6h, 12h, and 24h, or with 10uM GNE-140 (LDHA/B inhibitor) for 24h. **g,** Histone Kla and Kac levels were analyzed by immunoblots 24h-post LPS/IFNγ activation, with or without replenishing fresh media (containing LPS/IFNγ or not) every 4h. **h**, BMDM cells were stimulated with PBS (M0), LPS/IFNγ (M1), and interleukin-4 (M2) for 24 hours, respectively. Intracellular lactate was measured using a lactate colorimetric kit. Graphs show mean with s.e.m. from three biological independent samples; statistical significance was determined using one-way ANOVA followed by Dunnett's multiple comparisons test. **i, j,** Antibody specificity was evaluated by ChIP-qPCR. Competition was carried out by pre-incubating the indicated antibodies with a 10-fold excess of corresponding peptides. **k,** H3K18la antibody specificity was shown by full immunoblot using total lysate from MCF-7 cells with or without 10mM

sodium L-lactate treatment for 24h. **l,** H3K18la and H3K18ac are enriched in promoter regions. The promoter was defined as regions ± 2 kb around known transcription start sites. **m, n,** H3K18la and H3K18ac correlate with steady-state mRNA levels. The average ChIP signal intensity (read count per million mapped reads) for indicated antibodies is shown for genes with different expression levels (top 25%, the second 25%, the third 25%, and the bottom 25% of RNA-seq counts). **o, p,** IGV tracks for *Arg1* and *Crem* from ChIP-seq study, representing data from single experiment. **a–f,** Data represent two independent experiments. **g, i–k,** Data represent three independent experiments.

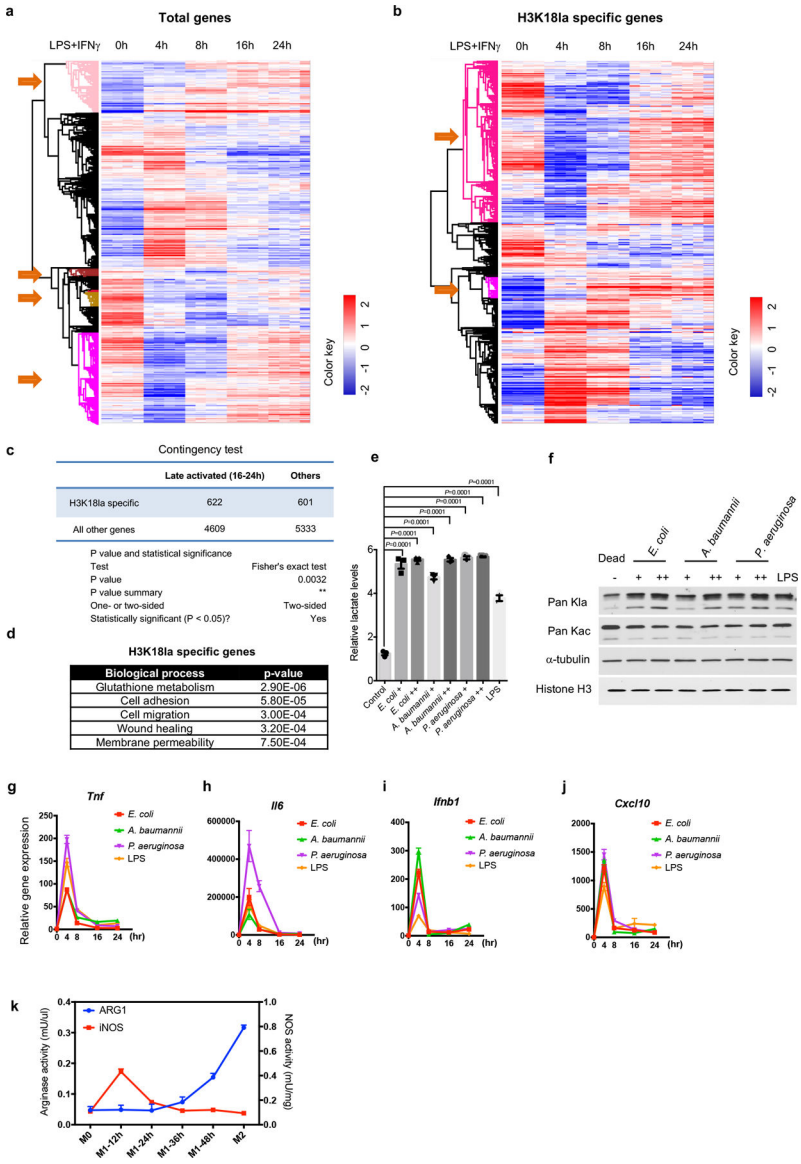

Extended Data Figure 5. Histone Kla specific genes are associated with late activated M2-like gene expression.

a, b, Heatmaps showing expression kinetics of total genes (**a**) and H3K18la-specific genes (**b**) during M1 macrophage polarization. N=4 biological replicates. The color key represents log2 transformed fold change relative to the mean of each row. Arrows next to the heatmaps refer to late activated genes (16–24h) from H3K18la specific or total genes used for contingency test. **c,** Contingency table analysis (Fisher's exact tests) shows the relation between specific H3K18la enrichment (H3K18la log2 FC>=1 and H3K18ac log2 FC<=0.5) and late gene activation. **d,** Gene Ontology analysis (biological processes) of H3K18la-specific genes. Statistical significance was determined by the modified Fisher Exact P-Value (EASE score) using DAVID Bioinformatics Resources 6.8, n=1223 genes. **e-j,** BMDM cells were infected with indicated gram-negative bacteria for 24 hours. Intracellular lactate (**e**) and histone Kla levels (**f**) were measured 24h after bacterially challenge. **e,** N=3 biological replicates; statistical significance was determined using one-way ANOVA followed by

Dunnett's multiple comparisons test. **g-j,** Gene expression was analyzed by RT-qPCR for indicated time points after bacterially challenge. **k**, Activities of iNOS and ARG1 were analyzed by immunoblots and commercialized kits from BMDMs activated by the indicated stimuli. Graphs show mean with s.e.m. from three biological replicates. **f** and **k** represent three independent experiments.

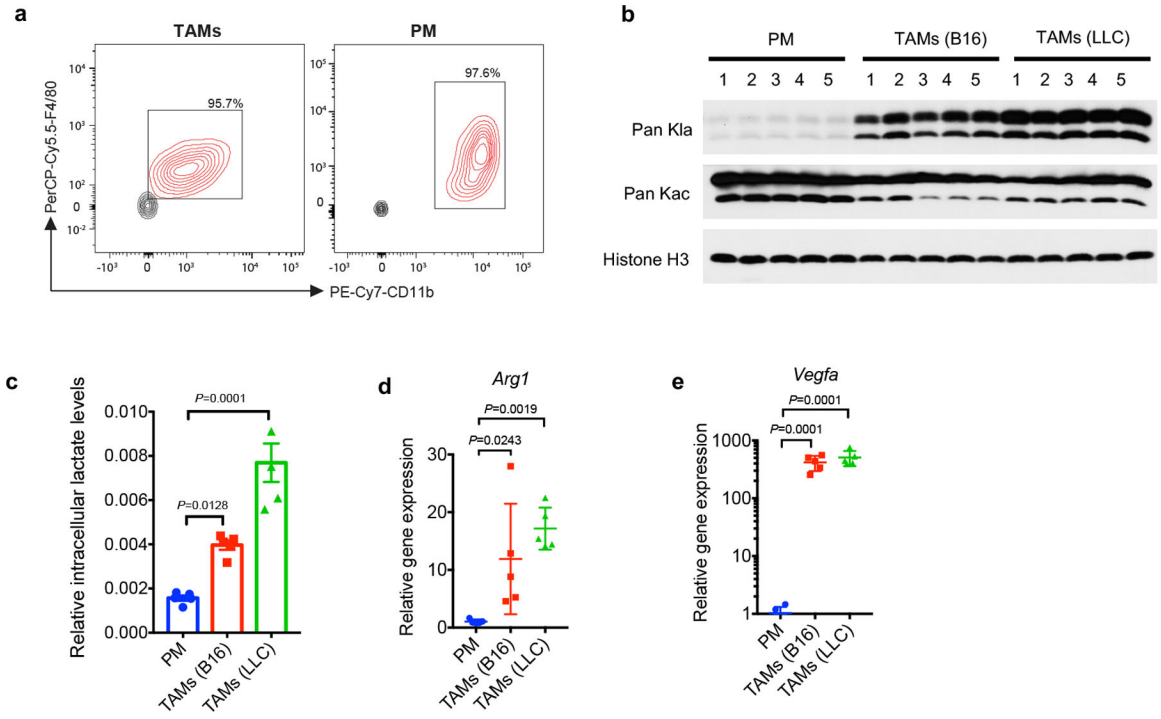

Extended Data Figure 6. Histone Kla levels are positively correlated with *Arg1* expression in tumor associated macrophages.

Tumor-associated macrophages (TAM) and Peritoneal macrophages (PMs) purify were confirmed by flow cytometry using *CD11b* (ThermoFisher Scientific, 25–0112) and *F4/80* (ThermoFisher Scientific, 17–4801) antibodies (**a**). Data were quantified by FlowJo v.10.4.1. Histone Kla and Kac levels were analyzed by immunoblots (**b**), intracellular lactate was measured using a lactate colorimetric assay kit (**c**), and gene expression of *Arg1* and *Vegfa* were analyzed by RT-qPCR (**d, e**) from FACS-sorted peritoneal macrophages (PM), TAMs within the tumor from LLC and B16 tumors. **c–e**, Graphs show mean with s.e.m. n=5 biological independent samples; statistical significance was determined using one-way ANOVA followed by Dunnett's multiple comparisons test. **a** and **b** represent five independent mice.

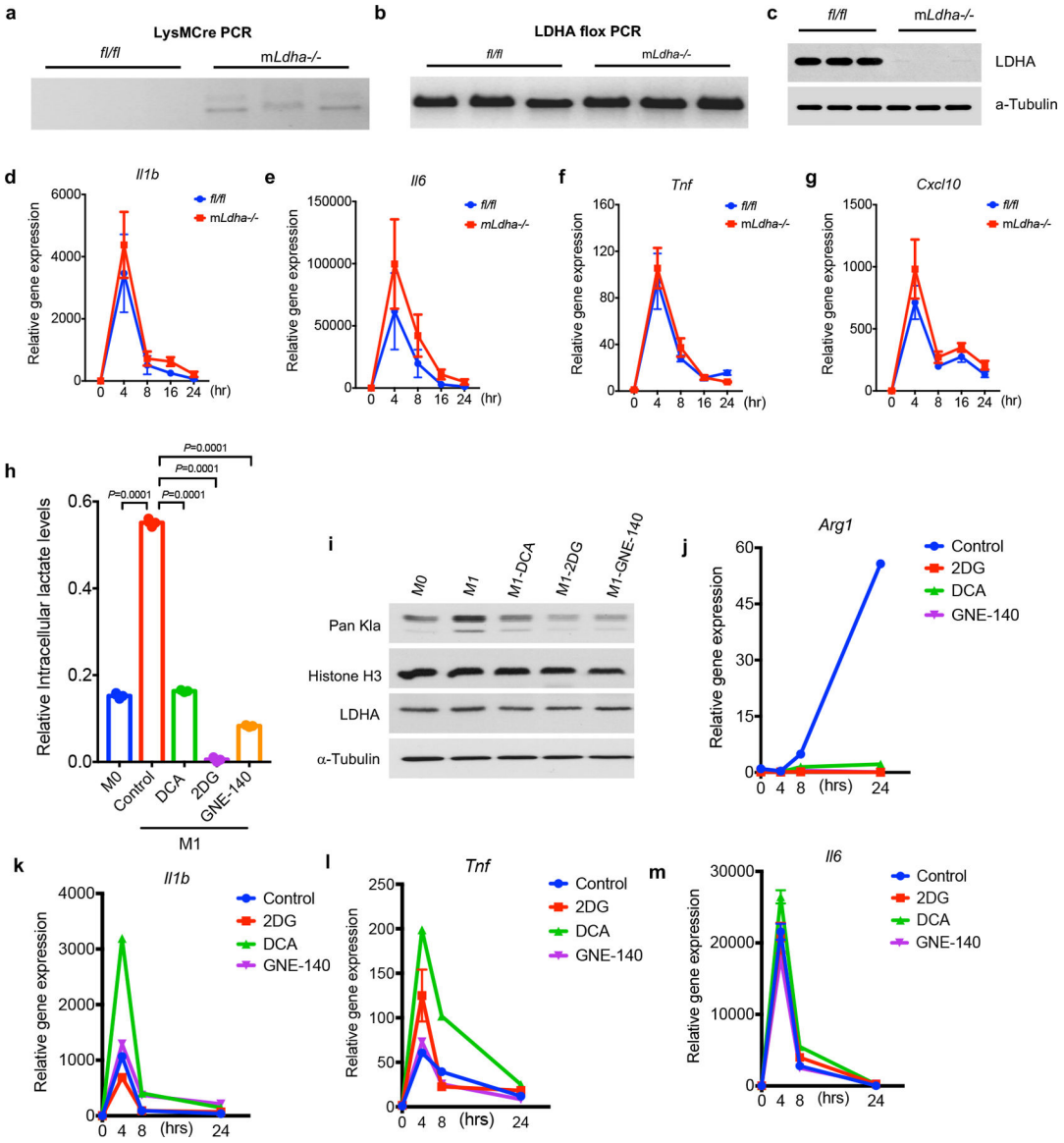

Extended Data Figure 7. Decreased lactate production lowered histone Kla levels and Arg1 expression during M1 polarization.

a, b, Genotyping of *Ldha*$^{fl/fl}$ × LysM-Cre$^{+/-}$ mice. **c,** Genotype validation by LDHA immunoblot analysis. **d–g,** Gene expression analysis of cytokines by RT-qPCR at indicated time points after M1 polarization. **h–m,** Intracellular lactate levels (**h**) were analyzed using a lactate colorimetric assay kit and global histone Kla levels (**i**) were measured by immunoblots 24h-post M1 polarization. Inhibitors were treated 30min after M1 polarization. Gene expression was analyzed by RT-qPCR at indicated time points after M1 polarization (**j–m**). Graphs show mean with s.e.m. from three biological replicates. **g**, statistical significance was determined using one-way ANOVA followed by Dunnett's multiple comparisons test. **a**, **b**, **c** and **i** represent three independent experiments.

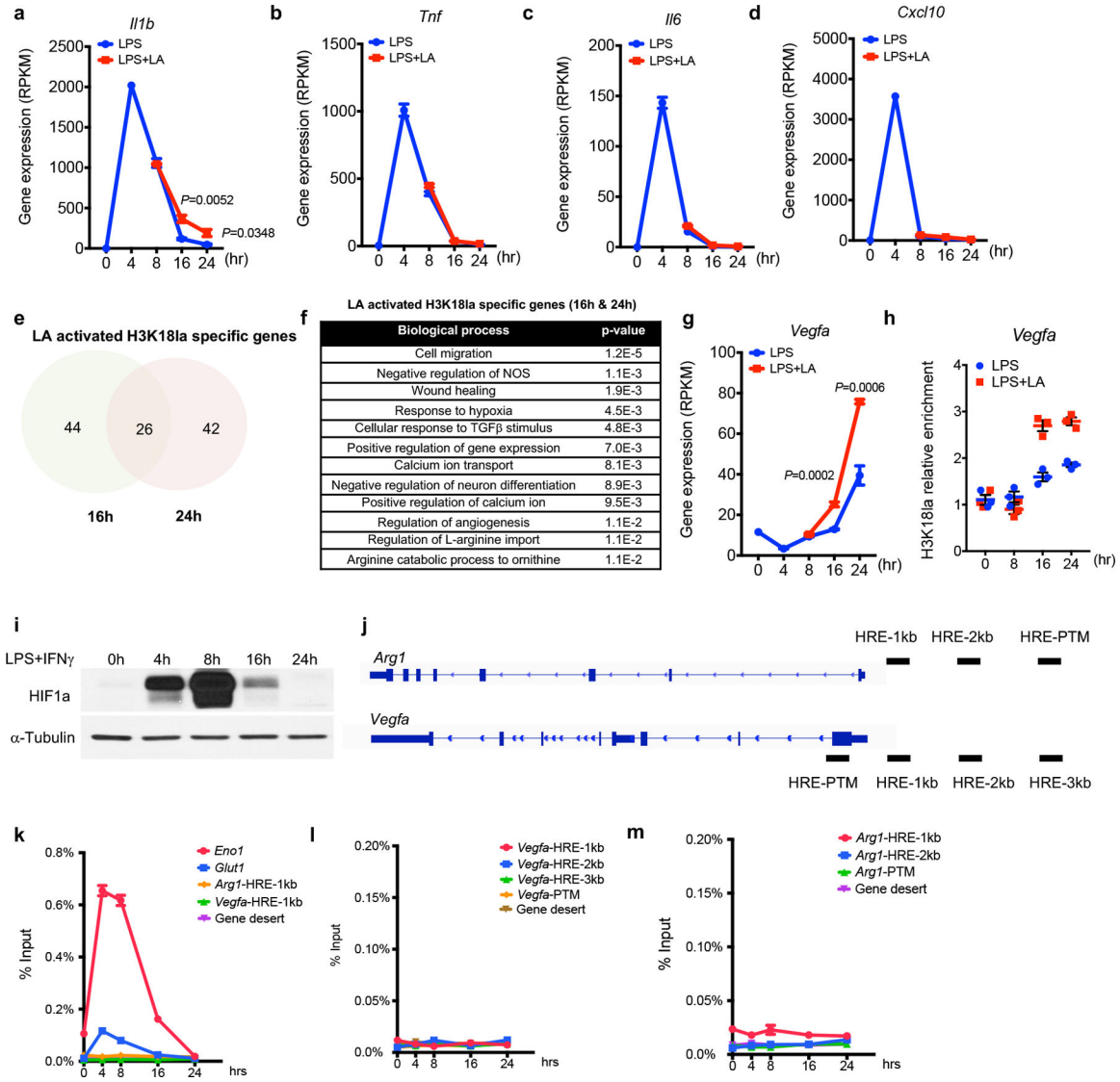

Extended Data Figure 8. Exogenous lactate activates M2-like gene expression through histone Kla.

a–d, Exogenous lactate (LA) does not interfere with gene expression of inflammatory cytokines. Results are shown as mean ± s.e.m. from four biological replicates. RPKM: Reads Per Kilobase of transcript per Million mapped reads (RPKM). **e,** Number of lactate-activated H3K18la-specific genes at indicated times are shown in a Venn diagram. **f,** Gene Ontology analysis (biological processes) of LA-induced H3K18la-specific genes at 16 and 24 h post-M1 polarization. Statistical significance was determined by the modified Fisher Exact P-Value (EASE Score) using DAVID Bioinformatics Resources 6.8, n=112 genes. **g,** *Vegfa* was induced by exogenous lactate during M1 macrophage polarization; n=4 biological replicates; statistical significance was determined using Multiple t tests corrected using Holm-Sidak method. **h,** H3K18la occupancy at *Vegfa* promoter was analyzed by ChIP-qPCR at indicated time and treatment; data represent three technical replicates from pooled samples. **i–m,** HIF1a is not required for histone Kla mediated *Arg1* induction during M1 polarization. **i,** Immunoblot of HIF1a at indicated time points post-M1 polarization. **j,**

Illustration of genomic loci targeted by *Arg1* and *Vegfa* ChIP-qPCR primers. HRE indicates regions containing the putative HIF1a binding motif “acgtg”. **k–m,** ChIP-qPCR analysis of HIF1a binding to indicated genomic locations; data represent three technical replicates from pooled samples. Graphs show mean with s.e.m. **i,** Data represent three independent experiments.

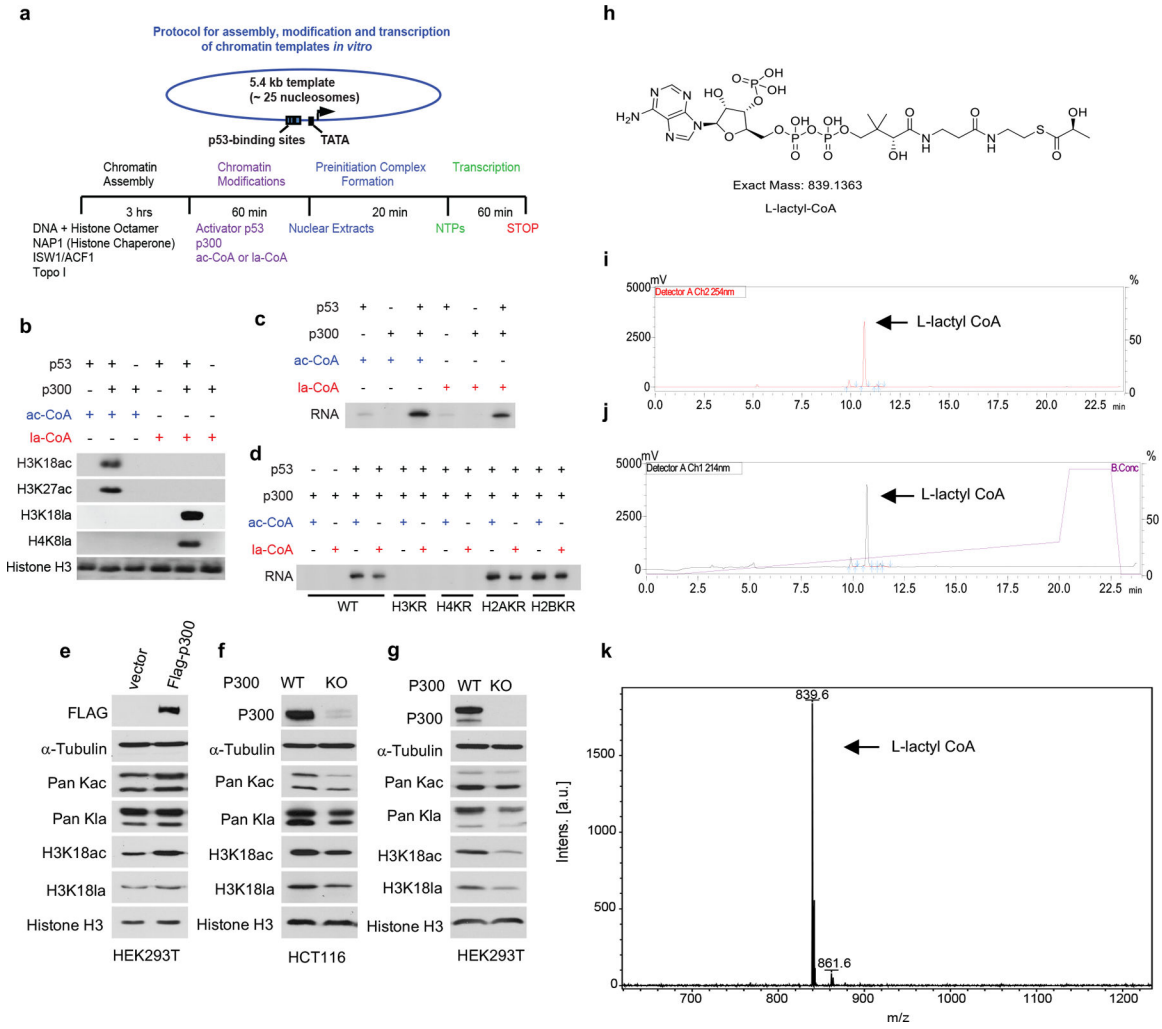

Extended Data Figure 9. Histone Kla directly stimulates gene transcription from recombinant chromatin *in vitro*.

a, Protocol for assembly, modification and transcription of chromatin templates. **b,** P300 catalyzes histone lactylation in a p53-dependent manner. **c,** Histone lactylation directly stimulates p53-dependent transcription from recombinant chromatin. **d,** H3 and H4 KR mutations eliminate p300-dependent transcriptional activation by p53. Recombinant chromatin was assembled with wildtype or H3KR, H4KR, H2AKR or H2BKR mutant histones as indicated. **e,** HEK293T cells were transfected with vector or FLAG-p300 plasmid. At 48-hr post-transfection, whole cell lysates were prepared and immunoblotted with indicated antibodies. **f, g**, Immunoblots of histone Kla and Kac levels in HCT116 (**f**) and HEK293T cells (**g**) where p300 was genetically deleted. **h–k,** Quality control of synthesized L-lactyl-CoA. **h,** Illustration of L-lactyl-CoA structure. **i, j,** HPLC analysis of the synthesized L-lactyl-CoA. UV detection wavelength was fixed at 214 and 254 nm. **k,** MALDI-Mass spectrometry analysis of L-lactyl-CoA. **b–g, i–k,** Data represent three independent experiments.

Supplementary Material

Refer to Web version on PubMed Central for supplementary material.

Acknowledgements.

HEK293T p300 KO cells were generously provided by Xiaoling Li lab at NIH. We thank Saadi Khochbin at Université Grenoble Alpes in Grenoble, France for brain storming and critically reading of this manuscript. We appreciate Kyle Delaney, and all other members in the Zhao lab and Becker lab for great discussions and technical support. This work was supported by the University of Chicago, Nancy and Leonard Florsheim family fund (Y.Z.), NIH grants R01GM115961, R01DK118266 (Y.Z.), R01DK102960, R01HL137998 (L.B.), R01CA129325 and R01DK071900 (R.G.R.).

References:

1. Pavlova NN & Thompson CB The Emerging Hallmarks of Cancer Metabolism. Cell Metab 23, 27–47, 10.1016/j.cmet.2015.12.006 (2016). [PubMed: 26771115]
2. Palsson-McDermott EM & O'Neill LA The Warburg effect then and now: from cancer to inflammatory diseases. Bioessays 35, 965–973, 10.1002/bies.201300084 (2013). [PubMed: 24115022]
3. Sabari BR, Zhang D, Allis CD & Zhao YM Metabolic regulation of gene expression through histone acylations. Nat Rev Mol Cell Bio 18, 90–101, 10.1038/nrm.2016.140 (2017). [PubMed: 27924077]
4. Kaelin WG Jr. & McKnight SL Influence of metabolism on epigenetics and disease. Cell 153, 56–69, 10.1016/j.cell.2013.03.004 (2013). [PubMed: 23540690]
5. Tan M et al. Identification of 67 histone marks and histone lysine crotonylation as a new type of histone modification. Cell 146, 1016–1028, 10.1016/j.cell.2011.08.008 (2011). [PubMed: 21925322]
6. Liu X et al. Acetate Production from Glucose and Coupling to Mitochondrial Metabolism in Mammals. Cell 175, 502–513 10.1016/j.cell.2018.08.040 (2018). [PubMed: 30245009]
7. Semenza GL Oxygen sensing, hypoxia-inducible factors, and disease pathophysiology. Annual review of pathology 9, 47–71, 10.1146/annurev-pathol-012513-104720 (2014).
8. Haas R et al. Intermediates of Metabolism: From Bystanders to Signalling Molecules. Trends Biochem Sci 41, 460–471, 10.1016/j.tibs.2016.02.003 (2016). [PubMed: 26935843]
9. Martinez-Outschoorn UE et al. Ketones and lactate increase cancer cell "stemness," driving recurrence, metastasis and poor clinical outcome in breast cancer: achieving personalized medicine via Metabolo-Genomics. Cell Cycle 10, 1271–1286, 10.4161/cc.10.8.15330 (2011). [PubMed: 21512313]
10. Galvan-Pena S & O'Neill LA Metabolic reprograming in macrophage polarization. Front Immunol 5, 420, 10.3389/fimmu.2014.00420 (2014). [PubMed: 25228902]
11. Allis CD & Jenuwein T The molecular hallmarks of epigenetic control. Nat Rev Genet 17, 487–500, 10.1038/nrg.2016.59 (2016). [PubMed: 27346641]
12. Rath M, Muller I, Kropf P, Closs EI & Munder M Metabolism via Arginase or Nitric Oxide Synthase: Two Competing Arginine Pathways in Macrophages. Front Immunol 5, 532, 10.3389/fimmu.2014.00532 (2014). [PubMed: 25386178]
13. Colegio OR et al. Functional polarization of tumour-associated macrophages by tumour-derived lactic acid. Nature 513, 559–563, 10.1038/nature13490 (2014). [PubMed: 25043024]
14. An W, Kim J & Roeder RG Ordered cooperative functions of PRMT1, p300, and CARM1 in transcriptional activation by p53. Cell 117, 735–748, 10.1016/j.cell.2004.05.009 (2004). [PubMed: 15186775]
15. Tang ZY et al. SET1 and p300 Act Synergistically, through Coupled Histone Modifications, in Transcriptional Activation by p53. Cell 154, 297–310, 10.1016/j.cell.2013.06.027 (2013). [PubMed: 23870121]
16. Tannahill GM et al. Succinate is an inflammatory signal that induces IL-1 beta through HIF-1 alpha. Nature 496, 238-10.1038/nature11986 (2013). [PubMed: 23535595]

17. Walenta S et al. High lactate levels predict likelihood of metastases, tumor recurrence, and restricted patient survival in human cervical cancers. Cancer Res 60, 916–921 (2000). [PubMed: 10706105]
18. Kratz M et al. Metabolic dysfunction drives a mechanistically distinct proinflammatory phenotype in adipose tissue macrophages. Cell Metab 20, 614–625, 10.1016/j.cmet.2014.08.010 (2014). [PubMed: 25242226]
19. Shechter D, Dormann HL, Allis CD & Hake SB Extraction, purification and analysis of histones. Nat Protoc 2, 1445–1457, 10.1038/nprot.2007.202 (2007). [PubMed: 17545981]
20. Cox J & Mann M MaxQuant enables high peptide identification rates, individualized p.p.b.-range mass accuracies and proteome-wide protein quantification. Nat Biotechnol 26, 1367–1372, 10.1038/nbt.1511 (2008). [PubMed: 19029910]
21. Kim D, Langmead B & Salzberg SL HISAT: a fast spliced aligner with low memory requirements. Nat Methods 12, 357–360, 10.1038/nmeth.3317 (2015). [PubMed: 25751142]
22. Robinson MD, McCarthy DJ & Smyth GK edgeR: a Bioconductor package for differential expression analysis of digital gene expression data. Bioinformatics 26, 139–140, 10.1093/bioinformatics/btp616 (2010). [PubMed: 19910308]
23. Huang DW, Sherman BT & Lempicki RA Systematic and integrative analysis of large gene lists using DAVID bioinformatics resources. Nature Protocols 4, 44–57, 10.1038/nprot.2008.211 (2009). [PubMed: 19131956]
24. Huang DW, Sherman BT & Lempicki RA Bioinformatics enrichment tools: paths toward the comprehensive functional analysis of large gene lists. Nucleic Acids Research 37, 1–13, 10.1093/nar/gkn923 (2009). [PubMed: 19033363]
25. Cuddapah S et al. Native chromatin preparation and Illumina/Solexa library construction. Cold Spring Harb Protoc 2009, 10.1101/pdb.prot5237 (2009).
26. Langmead B & Salzberg SL Fast gapped-read alignment with Bowtie 2. Nat Methods 9, 357–359, 10.1038/nmeth.1923 (2012). [PubMed: 22388286]
27. Langmead B, Trapnell C, Pop M & Salzberg SL Ultrafast and memory-efficient alignment of short DNA sequences to the human genome. Genome Biol 10, R25, 10.1186/gb-2009-10-3-r25 (2009). [PubMed: 19261174]
28. Li H et al. The Sequence Alignment/Map format and SAMtools. Bioinformatics 25, 2078–2079, 10.1093/bioinformatics/btp352 (2009). [PubMed: 19505943]
29. Zhang Y et al. Model-based analysis of ChIP-Seq (MACS). Genome Biol 9, R137, 10.1186/gb-2008-9-9-r137 (2008). [PubMed: 18798982]
30. Liao Y, Smyth GK & Shi W featureCounts: an efficient general purpose program for assigning sequence reads to genomic features. Bioinformatics 30, 923–930, 10.1093/bioinformatics/btt656 (2014). [PubMed: 24227677]
31. Perez-Riverol Y et al. The PRIDE database and related tools and resources in 2019: improving support for quantification data. Nucleic Acids Res 47, D442–D450, 10.1093/nar/gky1106 (2019). [PubMed: 30395289]

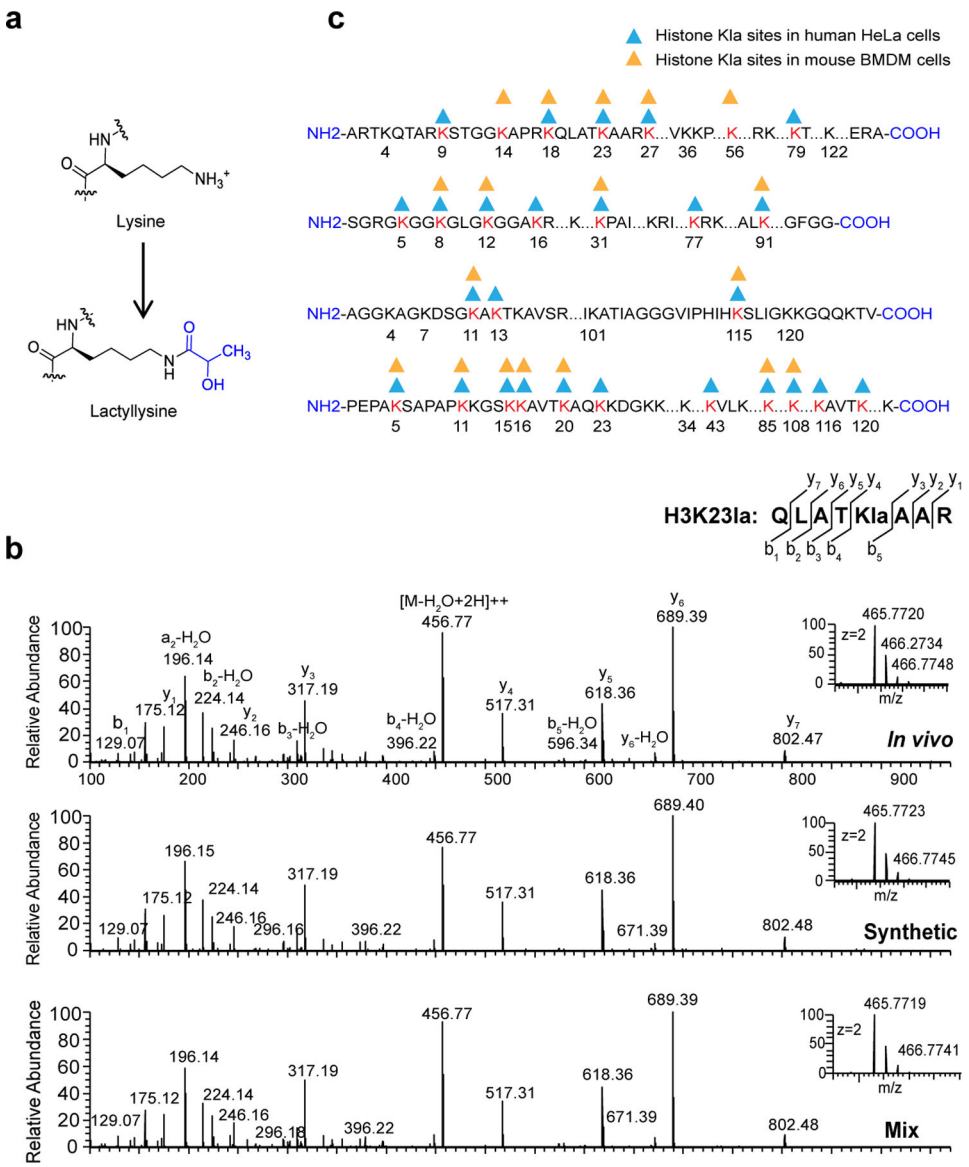

Figure 1. Identification and validation of histone Kla.

a, Illustration of Kla structure. **b,** MS/MS spectra of a lactylated histone peptide (H3K23la) derived from MCF-7 cells (*in vivo*), its synthetic counterpart, and their mixture. b-ion refers to the amino-terminal parts of the peptide and y-ion refers to the carboxy-terminal parts of the peptide. Data represent two independent experiments. **c,** Illustration of histone Kla sites identified in human and mouse cells.

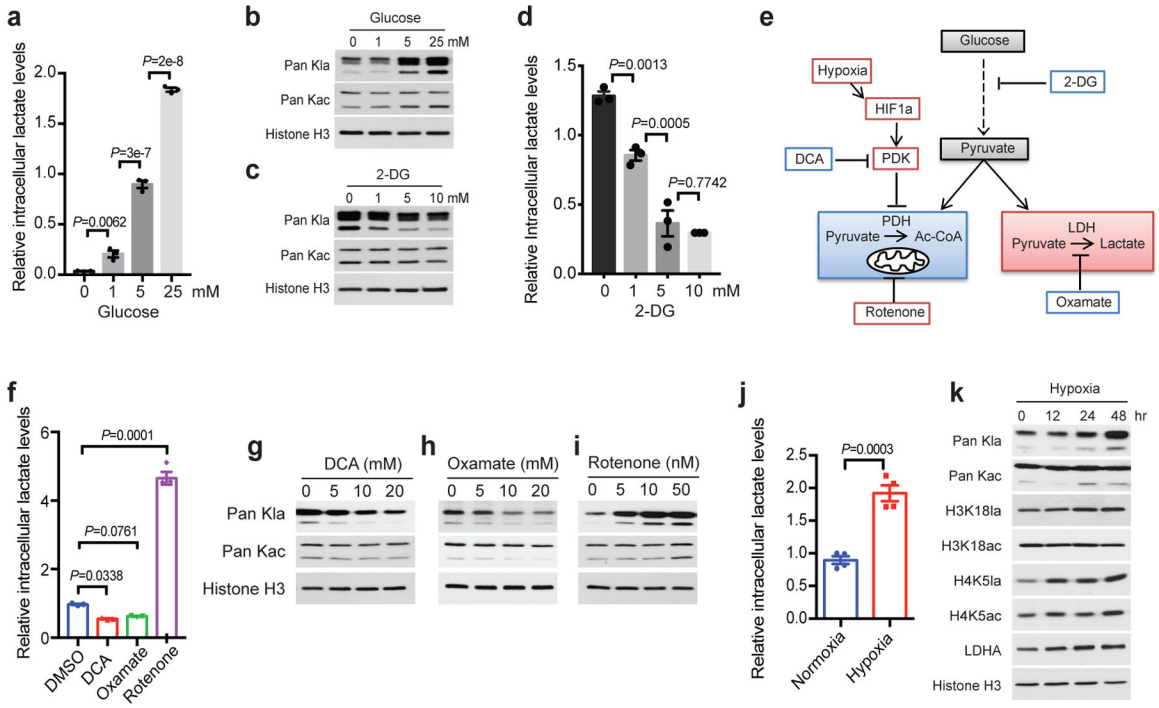

Figure 2. Lactate regulates histone Kla.

Intracellular lactate (**a** and **d**) and histone Kla levels (**b** and **c**) were measured from MCF-7 cells cultured in different glucose concentrations or different 2-DG concentrations in the presence of 25mM glucose for 24 hours. Lactate was measured by a lactate colorimetric kit; n=3 biological replicates; statistical significance was determined using one-way ANOVA followed by Sidak's multiple comparisons test. Immunoblots was carried out using acid-extracted histone samples. The pan anti-Kla and anti-Kac immunoblots indicate molecular weights between 10kD and 15kD. **e,** Regulation of glycolysis and lactate production by diverse metabolic modulators. **f,** Intracellular lactate levels were measured in MCF-7 cells treated with indicated glycolysis modulators for 24 hours. N=3 biological replicates; statistical significance was determined using one-way ANOVA followed by Dunnett's multiple comparisons test. **g-i,** Immunoblots of acid extracted histones (Rotenone and DCA) or whole cell lysates (Oxamate) from MCF-7 cells in response to different glycolysis modulators. **j,** Intracellular lactate levels were measured in MCF-7 cells in response to hypoxia. N=4 biological replicates; statistical significance was determined using unpaired t test (Two-tailed). **k,** Immunoblots of acid extracted histones from MCF-7 cells under hypoxia (1% oxygen) for indicated time points. **a, d, f, j,** Graphs show mean with s.e.m. **b, c, g, h, i, k,** Data represent three independent experiments.

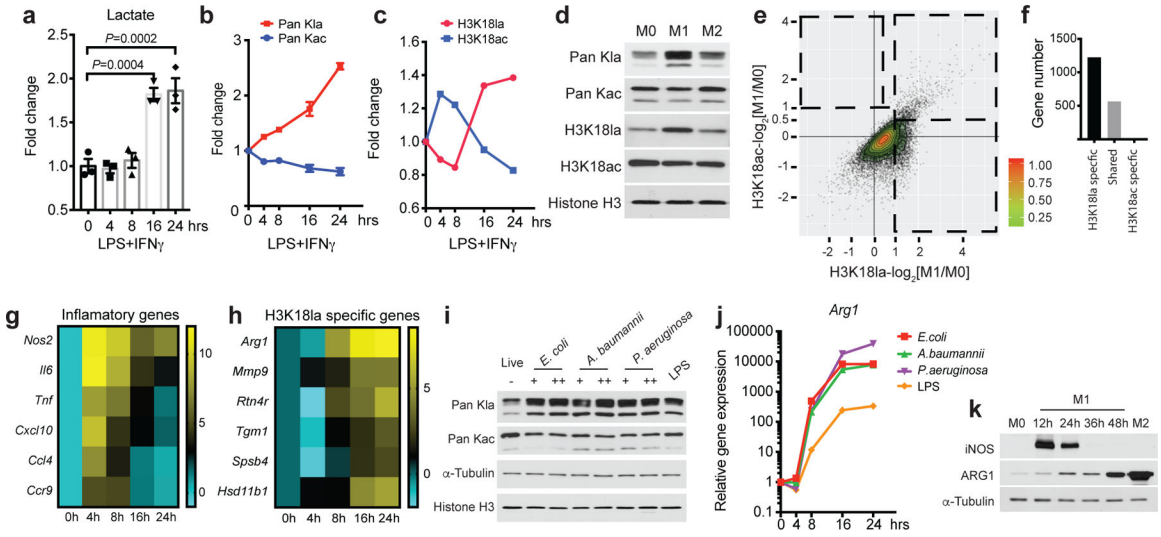

Figure 3. Elevated Histone Kla during M1 macrophage polarization is associated with M2-like gene activation.

a-c, Bone marrow-derived macrophages (BMDMs) were activated with LPS+IFNγ. Intracellular lactate (**a**) was measured using a lactate colorimetric kit. N=3 biological replicates; statistical significance was determined using one-way ANOVA followed by Dunnett's multiple comparisons test. Histone acylations were analyzed by immunoblots using whole cell lysates (**b, c**). ImageJ was used for quantification; n=3 technical replicates. Data represent two independent experiments. **d,** BMDM cells were stimulated with PBS (M0), LPS+IFNγ (M1), and interleukin-4 (M2) for 24 hours, respectively. Acid-extracted histones were used for immunoblots. **e, f,** Scatter plot (**e**) and bar plot (**f**) showing genes with promoters marked by exclusively elevated H3K18la (H3K18la-log$_2$[M1/M0] ≥1 and H3K18ac-log$_2$[M1/M0] ≤0.5, H3K18la-specific), elevated in both H3K18la and H3K18ac (H3K18la-log$_2$[M1/M0] ≥1 and H3K18ac-log$_2$[M1/M0] ≥0.5, shared), or exclusively elevated H3K18ac (H3K18ac-log$_2$[M1/M0] ≥1 and H3K18la-log$_2$[M1/M0] ≤0.5, H3K18ac-specific). **g, h,** Heat maps showing gene expression kinetics (using Reads Per Kilobase of transcript per Million mapped reads (RPKM) values from RNA-seq) of exemplar inflammatory genes (**g**) and H3K18la-specific genes (**h**). The color key represents log2 transformed fold change relative to gene expression at 0h. N=4 biological replicates. **i, j,** BMDM cells were infected with indicated Gram-negative bacteria or LPS, respectively. Histone Kla levels were measured by immunoblots (**i**) at 24h after bacterial challenge. "+" indicates lower dose and "++" indicates higher dose. Gene expression were analyzed by RT-qPCR (**j**) at indicated time points post bacterial challenge. N=3 biological replicates. **k,** Protein levels of iNOS and ARG1 were analyzed by immunoblots from BMDMs activated by the indicated stimuli. **a, b, c, j,** Graphs show mean with s.e.m. **d, i, k,** Data represent three independent experiments.

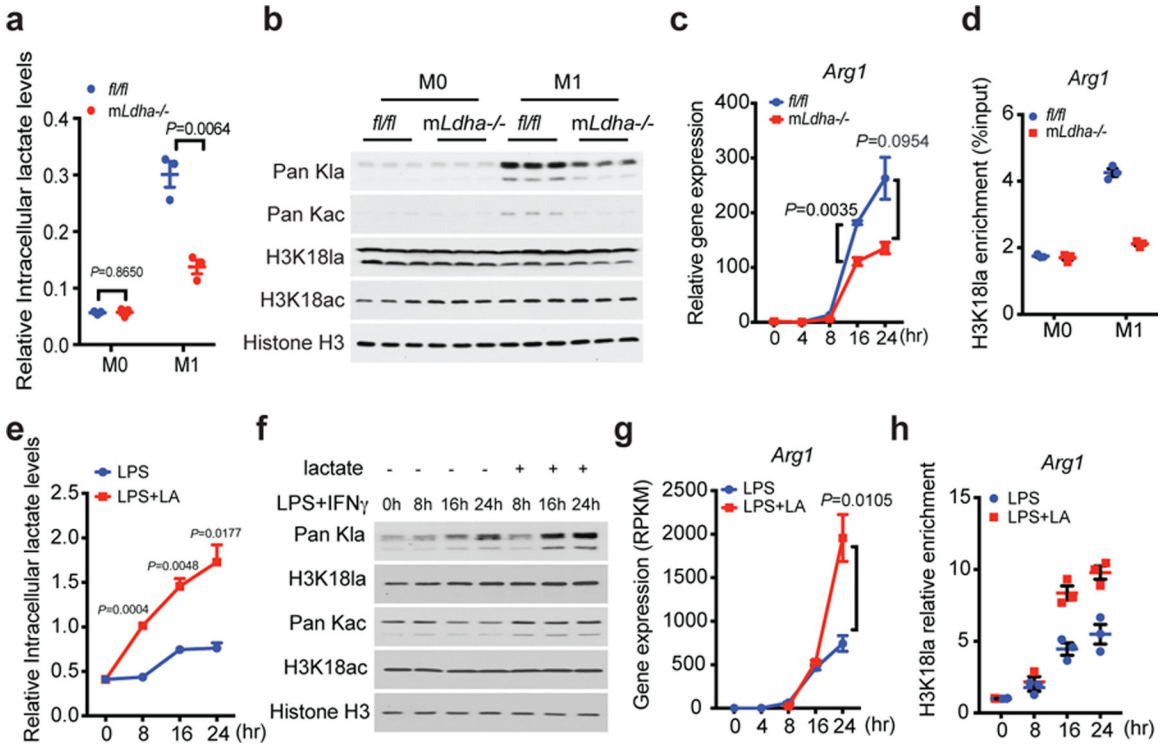

Figure 4. Lactate activates M2-like gene expression through histone Kla.

a–d, Decreased lactate production in LDHA deficient (myeloid specific *Ldha*$^{-/-}$) BMDM cells resulted in lowered histone Kla levels and *Arg1* expression during M1 polarization. Intracellular lactate levels were measured using a lactate colorimetric kit (**a**) and global histone Kla levels were measured by immunoblots (**b**) 24h-post M1 polarization. **c,** Gene expression were analyzed by RT-qPCR at indicated time points after M1 polarization. **a–c,** N=3 biological replicates. **d**, H3K18la occupancy was analyzed by ChIP-qPCR 24h-post M1 polarization. Data represent three technical replicates from pooled samples. **e–h,** Exogeneous lactic acid (25 mM) was added to BMDM cells 4 h post-M1 polarization (LPS +IFNγ), and cells were collected at indicated time points post-M1 polarization for intracellular lactate measurement (**e**), histone Kla immunoblot analysis (**f**), gene expression analysis (**g**) and H3K18la occupancy analysis by ChIP-qPCR (**h**). **e,** N=3 biological replicates, **f,** Data represent three independent experiments. **g,** RPKM: Reads Per Kilobase of transcript per Million mapped reads (RPKM). N=4 biological replicates. **h,** Data represent three technical replicates from pooled samples. **a, c, d, e, g, h,** Graphs show mean with s.e.m; statistical significance was determined using Multiple t tests corrected using Holm-Sidak method (**a, c, e, g**).